University of Kentucky Master's Theses | Graduate School

2010

DESIGN AND DEVELOPMENT OF STRUCTURALLY FEASIBLE SMALL UNMANNED AERIAL VEHICLES

Rohit Reddy Tammannagari
University of Kentucky, trohitreddy@gmail.com

Recommended Citation

ABSTRACT OF THESIS

DESIGN AND DEVELOPMENT OF STRUCTURALLY FEASIBLE
ANTENNAS FOR DEPLOYMENT ON INFLATABLE WINGS OF
SMALL UNMANNED AERIAL VEHICLES

This study is focused on designing conformal antennas to be deployed with the inflatable wings for unmanned aerial vehicles (UAV). The main emphasis is on utilizing the structure of the wing to develop antennas for various frequency bands, while maintaining the wing's aerodynamic performance. An antenna modeler and optimizer software called 4NEC2 and a program called WIRECODE were used to design and determine the characteristics of the antennas. The effect of flexibility of the inflatable wing on the antenna characteristics during flight is also evaluated.

ROHIT REDDY TAMMANNAGARI

_____05/03/2010_____

DESIGN AND DEVELOPMENT OF STRUCTURALLY FEASIBLE
ANTENNAS FOR DEPLOYMENT ON INFLATABLE WINGS OF
SMALL UNMANNED AERIAL VEHICLES

By

Rohit Reddy Tammannagari

<u>Dr. William T. Smith</u>

Director of Thesis

<u>Dr. Stephen Gedney</u>

Director of Graduate studies

<u>05/03/2010</u>

Date

RULES FOR THE USE OF THESIS

Unpublished thesis submitted for the Master's degree and deposited in the University of Kentucky Library are as a rule open for inspection, but are to be used only with due regard to the rights of the authors. Bibliographical references may be noted, but quotations or summaries of parts may be published only with the permission of the author, and with the usual scholarly acknowledgments.

Extensive copying or publication of the dissertation in whole or in part also requires the consent of the Dean of the Graduate School of the University of Kentucky.

A library that borrows this dissertation for use by its patrons is expected to secure the signature of each user.

<u>Name</u>   <u>Date</u>

_____

_____

_____

_____

_____

_____

_____

THESIS

Rohit Reddy Tammannagari

The Graduate School

University of Kentucky

2010

DESIGN AND DEVELOPMENT OF STRUCTURALLY FEASIBLE ANTENNAS FOR DEPLOYMENT ON INFLATABLE WINGS OF SMALL UNMANNED AERIAL VEHICLES

THESIS

A thesis submitted in partial fulfillment of the requirements for the degree of Master of Science in Electrical Engineering in the college of Engineering at the University of Kentucky

By

Rohit Reddy Tammannagari

Lexington, Kentucky

Director: Dr. William T. Smith, Associate Professor of Electrical Engineering

Lexington, Kentucky

2010

DEDICATION
ToMy Parents

ACKNOWLEDGEMENTS

I would like to thank my advisor, Dr. William T. Smith, for guiding my throughout my research work. I would like to express my heartfelt gratitude to him for being patient with me. I appreciate all his assistance during the editing process of this thesis.

I would also like to thank Dr. Robert Adams and Dr. Yuming Zhang for serving on my thesis committee. I would like to specially thank Dr. Suzanne Smith for providing me with an inflatable wing and essential inputs.

I would also like to thank Mr.Prasanna Padmanabhan for imparting his knowledge in the field of Antenna design and for supporting me throughout my work. I want to thank my parents who supported, encouraged and loved me throughout my life.

TABLE OF CONTENTS

LIST OF TABLES

LIST OF FIGURES

CHAPTER 1 – INTRODUCTION

Unmanned aerial vehicles (UAVs) have been used for performing a multitude of operations with lower cost and risk than their manned counterparts. While fixed and deployable rigid wings have been used in the past, the use of inflatable wings for these vehicles is an active topic of interest due to their compact stowing capability. This thesis focuses on developing various antenna configurations which make use of the inflatable wing structure for providing reliable communication while retaining the features of an inflatable wing, such as compactness, flexibility and robust aerodynamic shape.

1.1 Background

The flexible wing evolution can be dated back to the 15th century and many successful and not so successful attempts have been made to use these wings in flight design. This section of the chapter reflects briefly on some of these attempts and improvements.

1.1.1 Primitive designs

The art of flexible wing design is as old as the thought of flying itself. Leonardo Da Vinci, the Renaissance man, spent a large chunk of time building wings based on the bat wing (see Figure 1.1). He was enthralled by the flapping mechanism of the bat wing during flight and had deduced the theory that the wings should have a fixed inner section and a flexible outer portion. He even observed that the inner section moved slowly when compared to the outer section and thus he used control cables maneuverable through handles to obtain this flapping action [1].
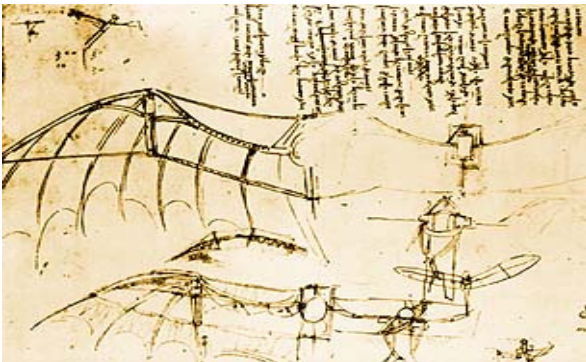
| (a) | (b) |

Figure 1.1: Primitive wing concepts (a) Da Vinci's early sketches of flexible wing concept, from [1]. (b) A design wing inscribed onto a bat wing

Da Vinci was one of the first people to study aerodynamic principles and design an ornithopter which is a flying aircraft using flapping wings (see Figure 1.2). In addition to this, there were a few notable attempts like the one by Edward Frost of Cambridge shire, England who built an ornithopter using willow, silk and feathers in 1902 [2].
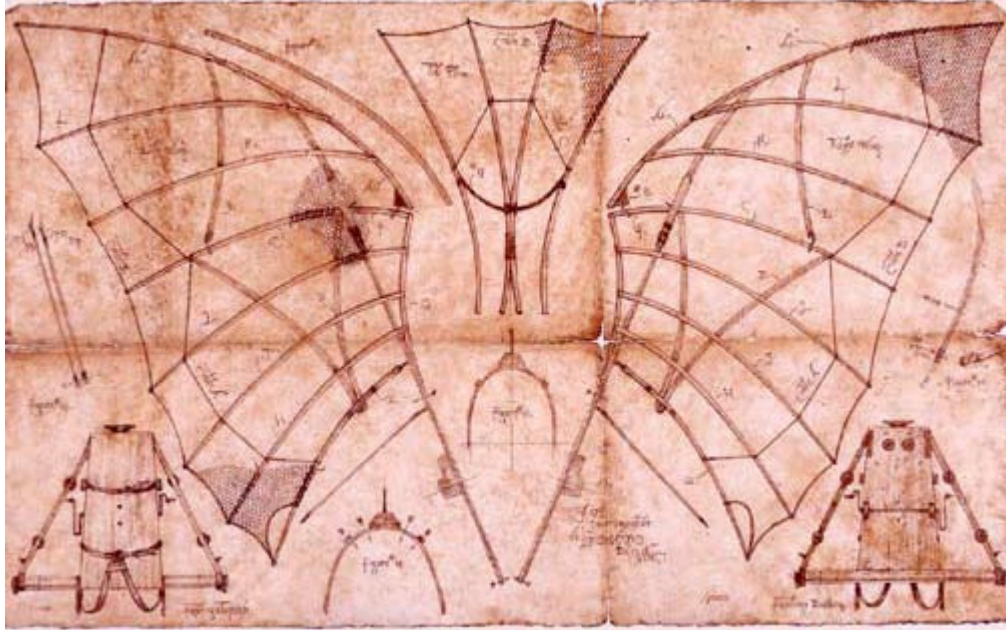
(a)

(b)

Figure 1.2: Primitive Ornithopter designs (a) Da Vinci's Ornithopter design based on a bat wing, from [1]. (b) Edward Frost's Ornithopter design, from [2].

Some success was achieved by James DeLaurier and his team at the University of Toronto aerospace studies in 2006 when they flew an ornithopter for 14 seconds covering a third of a kilometer at an average speed of 88kmph [2] (see Figure 1.3).

Figure 1.3: James DeLaurier and his team's practical Ornithopter, from [2].

1.1.2 Rigid deployable wings

The technology of deployable wings provided a scope for use in a lot of fields and military applications were the most important of all of them. This section deals with some of these applications. The production of aircraft using this concept grew rapidly, especially during the Second World War when there was a need of new technology and any possible aid to assist the ongoing war.

1.1.2.1 Jim Walker's folding-wing gliders

During the Second World War there was a shortage of supplies for the aviation industry and many companies had to cut down on production. The folding-wing glider, introduced in 1939 solely as a toy glider, was subsequently made use of by the Army for the purpose of providing practice for their anti-aircraft gunners. These glider models were used in infantry training centers, anti-aircraft training centers, tank destroyer schools, coast guard artillery schools and naval training stations by the allies.

In a short span of time a special military launcher was designed with the capability of catapulting the glider being used as an interceptor high into the air (see Figure 1.4). The interceptor would reach an altitude of 300 feet before deploying its wings and going in a glide mode. This glider, which acted as an interceptor, simulated a real plane with its twist and fold action. At that altitude and flight, it acted as a great moving target for the gunners located on the ground [3].

3
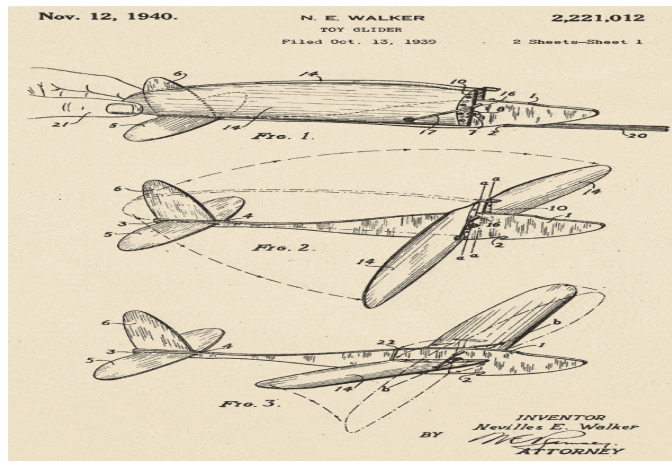
(a)

(b)

Figure 1.4: Jim walker's deployable wing concepts (a) Deployable wing concept of Walker from his Patent [3]. (b) A military launcher for Jim Walker's glider along with the gunners aiming at the interceptors in the air (can be seen in Figure), Fort Lewis, 1943, from [3].

1.1.2.2   Tube- Launched, Optically tracked, Wire-guided Missiles (TOW)

The tube- launch missiles which deploy wings and the rear stabilizers after leaving the launch tube were introduced in the 1970's. These wire –guided, optically tracked missiles are used in anti-armor, anti-bunker, anti-fortification and anti-amphibious landing roles. The early use of these missiles can be dated back to the Vietnam War in 1972 [4].

The modern counterparts of these missiles use foldable wings, fins and many mechanical modifications compared to their predecessors. This is a good example for the application of deployable wings in military operations.

1.1.2.3   Deployable Wing Planes

In post Second World War era, a lot of planes were designed making use of the deployable wing mechanism. In addition to these, private aircrafts too were built with deployable wings in a bid to maximize space savings by twisting and folding back the wings against the fuselage. Some of them have been presented in Figure 1.5 below.

(a)

(b)

(c)

Figure 1.5: Deployable wing planes (a) Douglas A-3 Skywarrior, (copyright by GlobalSecurity.org [5], reprinted with permission). (b) Mustang- A private plane, from [6]. (c) Shadow, from [7].

1.1.2.4 Wide Area Surveillance projectile (WASP)

The wide area surveillance projectile or simply the WASP is a small UAV and has been designed by a team at MIT and engineers from Draper laboratories. The UAV has the ability to get launched from a five inch gun and has a foldable wing, tail and propeller that can fit correctly into the fuselage. The small UAV deploys the wings and propellers upon reaching the point of interest. This aircraft is mainly aimed for providing quick surveillance as the name suggests. The deployment procedure has been described in the Figure 1.6 below [8].

(a)

(b)
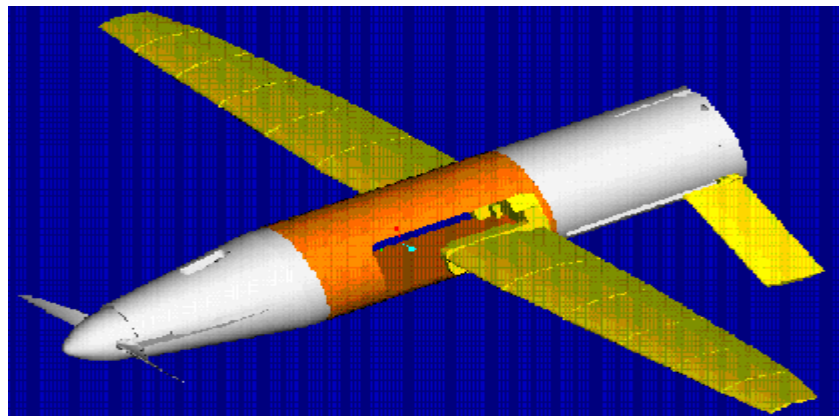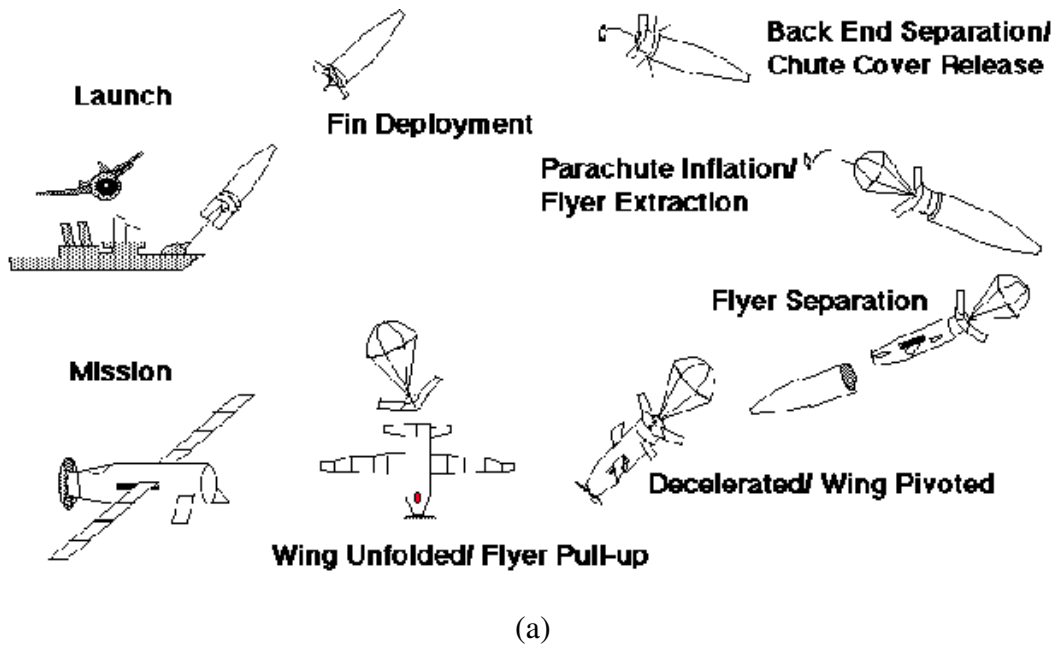
Figure 1.6: WASP design (a) Image of a WASP flyer, from [8]. (b) WASP wing deployment procedure, from [8].

The WASP can carry a navigation system, CCD camera and a transmitter and is usually placed in a shell [8]. Advanced composite materials were used for the wing design as they have a high stiffness -to- weight ratio. After tube- launched missiles, the gun-launched UAV'S were the next step and the WASP is one of those attempts involving deployment of wings and propellers that can fold out after the launch.

1.1.3 Inflatable Wings

Inflatable wing concepts have been in the picture since the 1930's and they have been used effectively for aircrafts since the 1950's. There are many variants of the basic designs in use

today and a lot of modified versions are yet to come. Some of the most successful inflatable airplanes during that period were designed by Goodyear Aerospace. The GA-33 inflatoplane designed in 1956 had a wing span of 22 feet and a length of 19 feet 7 inches. The vehicle had a cruise speed of 60mph and a range of 390mph.

The GA-466 inflatoplane was another vehicle designed by Goodyear during that period had a wing span of 28 feet and a length of 19 feet 2 inches. The vehicle had a cruise speed of 55mph and a range of 275mph. A total of twelve inflatoplanes were built by the Goodyear aerospace till 1972 and the project was terminated in 1973. ILC Dover made use of the inflatable wing technology in the 1970's and built the unmanned ILC Dover Apteron. The unmanned aircraft had a wingspan of 5.1 feet and weighed 7 lbs. It was very portable and had the capability of being launched remotely [9].

Inflatable wing technology has since then taken giant strides. The Big Blue project, which started in 2002 at the University of Kentucky, worked on the application of inflatable wings to be used on unmanned aerial vehicles for Mars exploration.

The basic idea was to go to Mars with a small package and to have relatively big wings in order to fly in the light atmosphere. An inflatable wing can be packed in a small volume and then can be opened up to be relatively large. Therefore these wings have proved that they are a better fit for mars airplanes covering surface area at lower altitudes than the satellites and Landers. The project proved that the wings can be used for deployment on NASA's Mars mission airplanes as they evenly distribute any physical impact (when a rock hits the wing etc…) over the entire area of the inflatable system without any damage [10].

1.2 Motivation

Inflatable wings used for unmanned aerial vehicles (UAV's) are packed, deployed and possibly rigidized as per requirement. This requires the antenna deployed on the wing to be flexible, conformal and should have the ability to provide reliable communication throughout the flight mission. Thus, the task of designing antennas on the wing is a pivotal one and has been the focus of this thesis.

1.3 Objectives

The focus of this thesis is to design a set of antenna modules which can be deployed with the inflatable wing structure. A few of these antennas operate at VHF and UHF radio frequencies and a special set of antennas called branch line planar antennas have been designed specially to operate at lower VHF range. These groups of antennas effectively make use of the structure of the wing as they run along the spars and wing surfaces and provide for being highly efficient. The other goals of this study are to check for the effect of wing flexing on the various antenna characteristics during the time of flight. The programs Wirecode and 4NEC2 were used to obtain the radiation patterns and current distributions of the antenna systems.

1.4 Contributions

The potential impact of this thesis can be in using the structure of the inflatable wings to design antennas. The thesis study has shown that antennas can be built by running them along the length and breadth of the wing along the spars thus making effective use of the wing design. This opens up the window for creating wide varieties of antennas which conformably integrate into any wing design. The area of branch line planar antennas for inflatable wings which operate at lower VHF range is another significant contribution of this thesis research for lower frequency bands. Because of its importance, an entire chapter has been dedicated to explain the guidelines of geometry and characteristics of these antennas. Also, the study throws light on the effect of flexibility on the antenna characteristics during flight and lays a solid documented groundwork on these effects.

1.5 Outline of the thesis

This thesis consists of seven chapters. This chapter provided a quick background of the evolution of deployable wings and how inflatable wings were shown to be applicable for NASA's Mars missions at the University of Kentucky. This chapter also outlined the motivations for this study, the objective of the research and the contributions of this work.

Chapter 2 explains all the theoretical concepts that are needed to do this study. A brief description of the antenna modeler and optimizer 4NEC2 and the program WIRECODE, which work on the principle of the method of moments (MOM), is also provided.

Chapter 3 gives a total description of the geometry and configuration of all the antenna modules that operate in the VHF, UHF and higher frequency range. These include the Dipole, Yagi, Bowtie, Tapered-slot and Maltese-cross antennas.

Chapter 4 presents branch line planar antennas which operate in the low VHF range. It deals with the antenna profile, guidelines to obtain antenna dimensions, variants of this module and other prominent features of this design.

Chapter 5 deals with the simulation results and comparison of results for antennas covered in the chapters 3 and 4.

Chapter 6 addresses the various effects of flexibility of the inflatable wing on the branch line antenna parameters.

Chapter 7 wraps up the thesis work by providing a summary and conclusion. Also, an insight into future implications of this work is presented.

CHAPTER 2- THEORY

2.1 Radiowave Propagation using antennas

Communication was achieved by electrical means with the introduction of telegraphy in the year 1844 and by telephony in the year 1878. Wireless telegraphy, which used electromagnetic radiation, was used for the purpose of communication in the year 1897, forty three years after Maxwell theoretically predicted their use. There are two types of communication systems the ones using transmission lines and the ones that use electromagnetic radiation with an antenna at the transmitting and receiving end.

In the systems using electromagnetic radiation, the transmitting antenna radiates the signal power into a substantial angular region of space. Out of this, only a small fraction of radiated power is intercepted by the receiving antenna. Thus, there is a substantial coupling loss between the transmitting and receiving antennas. For a small distance, communication using transmission lines is better than communication using electromagnetic radiation owing to a lesser loss but, beyond a certain distance, electromagnetic radiation is by far the best means of communication. In mobile communication services, such as ship-to-shore, between aircraft and control centers, between mobile land vehicles, and in satellite systems, transmission lines can't be used for obvious reasons. Also, in hostile terrain and environment, the transmission lines are not feasible for economic reasons. Thus, antennas are clearly one of the most essential components in communication systems [11].

Radio frequency refers to a part of electromagnetic radiation with frequency between 3 KHz to 300 GHz. Different parts of the radio spectrum are used for different radio technologies and applications. The radio spectrum is normally governed by the government body of the respective country and is normally sold to private operators who use it for cellular, television and other operations. Table 2.1 below gives a brief demarcation of this radio frequency spectrum and shows the commonly used frequency band designations. Also, Table 2.2 gives the microwave and millimeter frequency band designations. Though the newer letter designation has come into the picture, the older letter designations introduced in the mid1940's are still in common use.

Table 2.1 Radio Frequency Spectrum (retyped from [11])

Frequency band	Wavelength	Designation	Service Area
3-30 KHz	100km-10km	Very low frequency (VLF)	Sonar and Navigation
30-300 KHz	10km-1km	Low frequency (LF)	Navigational aids and radio beacons
300-3000 KHz	1km-100m	Medium frequency (MF)	AM broadcasting, direction finding and coast guard communication
3-30 MHz	100m-10m	High frequency (HF)	Telephone, telegraph, amateur radio, ship-to-coast communication
30-300 MHz	10m-1m	Very high frequency (VHF)	Television, FM broadcast, police, Taxicab mobile radio
300-3000 MHz	1m-100mm	Ultrahigh frequency (UHF)	Television, satellite communication and surveillance radar
3-30 GHz	100mm-10mm	Super-high frequency (SHF)	Airborne radar, microwave links and satellite communication
30-300 GHz	10mm-1mm	Extremely high frequency (EHF)	Radar and experimental studies

Table 2.2 Microwave Frequency Band Designation (retyped from [11])

Frequency	Old Designation	New Designation
500-1000 MHz	VHF	C
1-2 GHz	L	D
2-3 GHz	S	E
3-4 GHz	S	F
4-6 GHz	C	G
6-8 GHz	C	H
8-10 GHz	X	I
10-12.4 GHz	X	J
12.4-18 GHz	Ku	J
18-20 GHz	K	J
20-26.5 GHz	K	K
26.5-40 GHz	Ka	K

2.2 Antenna Theory

According to the Webster's dictionary an antenna is defined as "a usually metallic device (as a rod or wire) for radiating and receiving radio waves. In other words an antenna is nothing but a transitional structure between a guiding device (coaxial cable, hollow pipe etc.) and the free space and vice versa [12].

An antenna can also be described as a structure, usually made from a good conducting material, which is designed to have a shape and size such that it will efficiently radiate electromagnetic power. Thus an antenna is a structure on which time-varying currents can be excited with relatively large amplitude when the antenna is connected to a source by means of a transmission line or a waveguide. There are various structural shapes that can be used for an antenna. But, from a practical standpoint, structures that are simple and economical to fabricate are normally used. The minimum size of the antenna must be comparable to the wavelength in order to radiate efficiently [11].

2.3 Types of Antennas

The theory behind antenna analysis is based on Maxwell's equations. There are various antenna types and some common types have been discussed below.

2.3.1 Wire Antennas

The wire antennas are the most commonly used antennas and can be seen everywhere in the day- to-day world. The various shapes of antennas such as the dipole, loop and helix antennas come under this category (see Figure 2.1). These antennas can be seen on the buildings, automobiles, aircrafts, ships and spacecrafts. The loop antennas mentioned above can be in any shape ranging from a circular to a rectangular, square or elliptical shape. Generally the circular shape is preferred for a loop antenna because of its simplicity [12].
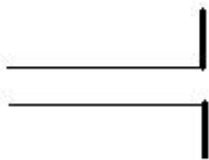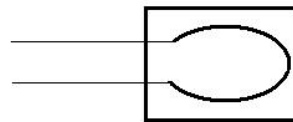
(a) Dipole   (b) Circular(square) loop

Figure 2.1: Basic Wire Antenna Configurations.

2.3.2 Aperture Antennas

The necessity to utilize the higher frequencies led to the use of the aperture antennas. These antennas are effectively used for aircraft and spacecraft applications because they can be effectively mounted with the skin of the aircraft and the spacecraft (see Figure 2.2). In order to protect them from hazardous conditions they can be conveniently covered by dielectric materials. These antennas are sophisticated are increasingly getting familiar to the layman day by day [12].

Figure 2.2: Aperture Antenna.

2.3.3 Microstrip Antennas

Microstrip antennas were one of the most prominent antennas for space applications in the early 1970's. As time has progressed they are being used for government and commercial applications. The geometry of these antennas consists of a metallic patch (mostly rectangular or circular) on a grounded substrate. They have low cross-polarization and good radiation characteristics. Also, they are easy to fabricate using modern printed-circuit technology, inexpensive, low profile and conformable to both planar and non-planar surfaces (see Figure 2.3). These antennas boast of being mechanically robust and very versatile in terms of resonant

frequency, polarization, pattern and impedance. These antennas are typically used on the spacecrafts, aircrafts, satellites, missiles, cars and also on handheld mobile telephones [12].
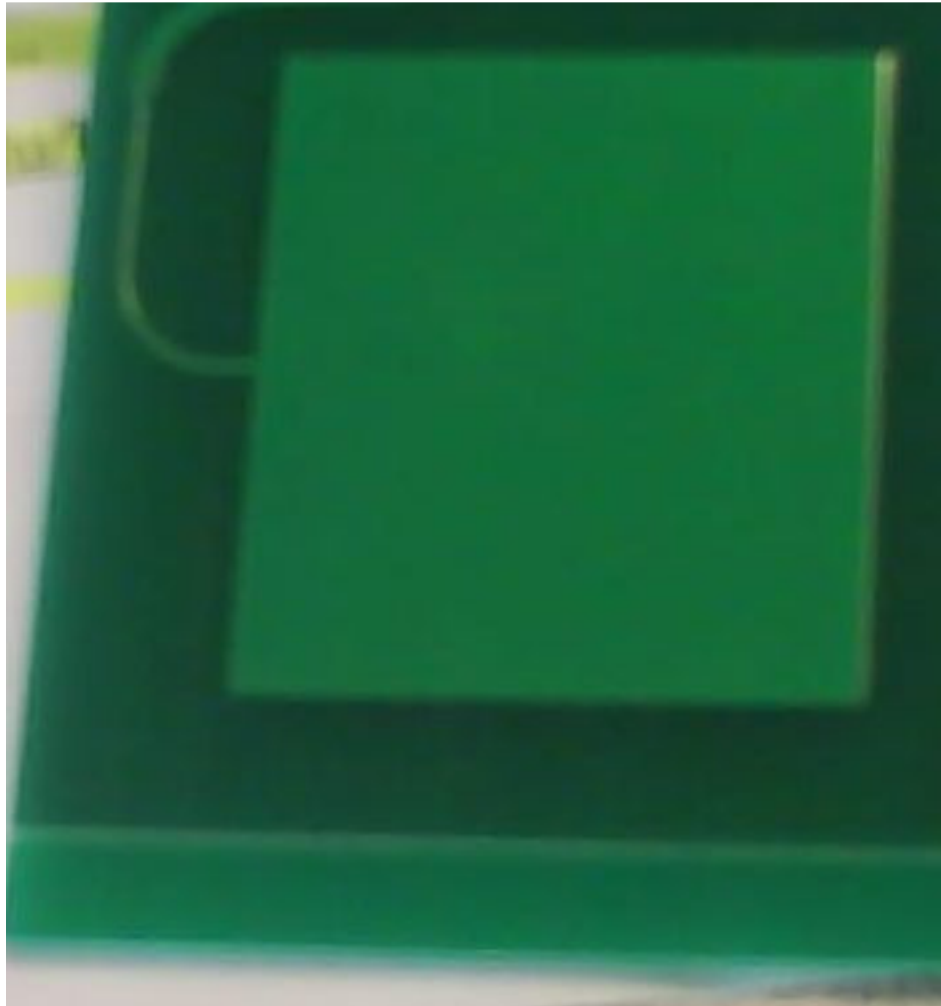
Figure 2.3: Microstrip Antenna.

2.3.4 Array Antennas

The radiation characteristics required by certain applications may not be obtained by using an individual antenna but maybe achieved using a set of antenna elements in a particular electric and geometric arrangement. This geometric arrangement of radiating elements is called an array antenna (see Figure 2.4). The radiation from all the individual elements adds up in a particular direction and gives a radiation maximum in a particular direction and a minimum in the other. An array, the individual elements are separated from each other in accordance with certain guidelines [12].

Figure 2.4: Antenna array configurations.

2.4 Radiation Pattern

The radiation pattern is the graphical representation of the radiation properties of an antenna as a function of the space coordinates [13] (see Figure 2.5). The radiation pattern is basically defined in the far-field region. The far field region is the region in which the radiated field exhibit localized plane wave behavior and the angular field distribution is independent of the distance from the antenna. A graph of the received electric field at a constant radius is referred to as the amplitude field pattern and the graph of the power density at a constant radius is referred to as the amplitude power pattern. The field and power patterns are normalized with respect to their maximum value so that its maximum value is never more than unity [12].
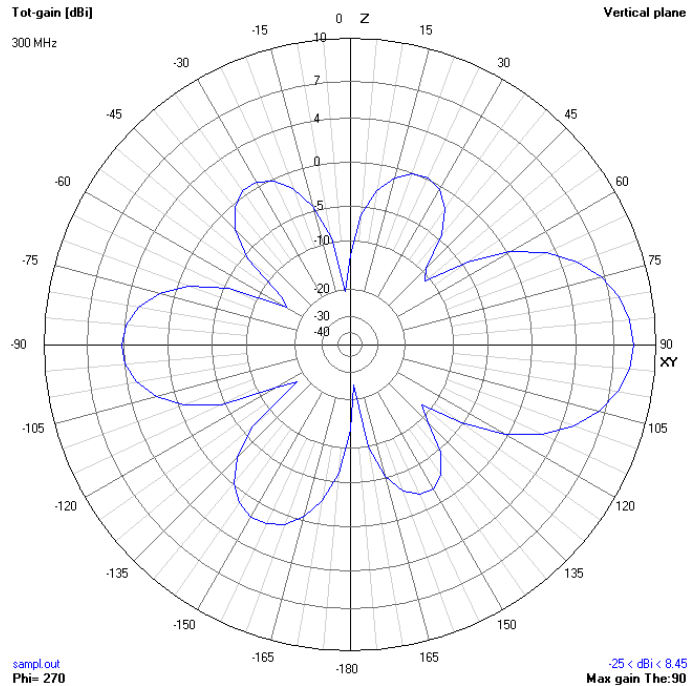
Figure 2.5: Radiation Pattern lobes, obtained using 4NEC2.

The radiation lobe is the portion of the radiation pattern surrounded by areas of very sparse intensity. The radiation lobe basically consists of the major and the minor lobes. The major lobes are the radiation lobes containing the direction of maximum radiation. The major lobes are also commonly called as the main lobes. Lobes other than the major lobes are referred to as the minor lobes, or side lobes. The back lobes are the ones which are located at an angle of 180 degrees with respect to the main beam axis. The radiation patterns are broadly classified as either isotropic or directional. An ideal antenna which radiates equally in all directions is referred to as an isotropic radiator. Though this type of antenna does not exist, in practice it is used as a reference for measuring the properties of other antennas. Likewise all the antennas which transmit and receive the electromagnetic waves efficiently in only a few directions are referred to as directional antennas. An antenna is said to have an Omni-directional pattern if it has a "non-directional pattern in a given plane and a directional pattern in an orthogonal plane" [12]. Thus the Omni-directional pattern is a special case of a directional pattern.

The antennas are also classified based on the type of radiation pattern. Antennas are either broadside or endfire (see Figure 2.6). A broadside antenna has the main beam maximum in a direction normal to the plane containing the antenna. An endfire antenna has the main beam maximum in a direction parallel to the plane containing the antenna [13].

16

dipole.out   Tot-gain   900 MHz
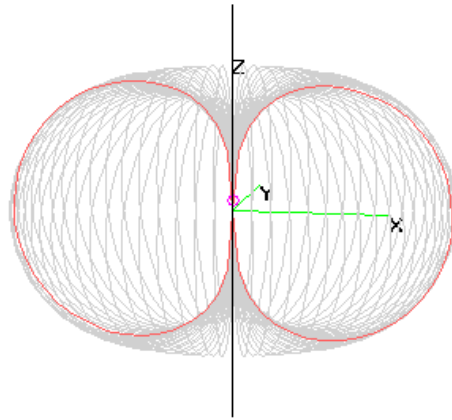
Theta : 80   Axis : 0.2 ft   Phi : 280

(a)

yagi.out   Tot-gain   900 MHz
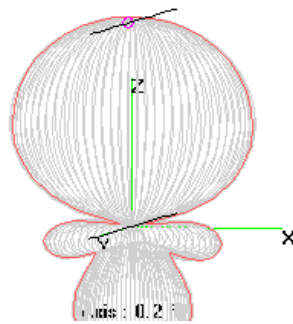
Theta : 94   Axis : 0.2 ft   Phi : 257

(b)

Figure 2.6: Polar plots of radiation pattern (Antenna is oriented along the z-axis) (a) Broadside radiation pattern. (b) Endfire radiation pattern, obtained using 4NEC2.

17

2.5 Radiation Intensity

The radiation intensity of an antenna in a given direction is basically defined as "power radiated per unit solid angle" [12]. The radiation intensity of an antenna is related to the far-zone electric field and can be described in the mathematical form as

$$U(\theta, \emptyset) = \frac{1}{2\eta} \left(\left| E_\theta^{ff}(\theta, \emptyset) \right|^2 + \left| E_\emptyset^{ff}(\theta, \emptyset) \right|^2 \right) \tag{2.1}$$

Here U is the radiation intensity and E(θ), E(Ø) represent the electric field components in the far-zone. η represents the intrinsic impedance of the medium. The total power is obtained by integrating the radiation intensity over the entire solid angle of 4π. The total power P_{rad} is

$$P_{rad} = \iint_{0\,0}^{2\pi\,\pi} U(\theta, \emptyset) \sin \theta \; d\theta \, d\emptyset \tag{2.2}$$

2.6 Beamwidth

The beamwidth is defined as the angular separation between two identical points on the opposite side of the pattern main beam [12]. The half-power beamwidth (HPBW) is defined by IEEE as "In a plane containing the direction of the maximum of a beam, the angle between the two directions in which the radiation intensity is one-half value of the beam" [12]. Also the angular separation between the first nulls of a pattern is referred to as the first-null beamwidth (FNBW).

2.7 Directivity

Directivity is one of the most important parameters of an antenna and it basically tells how much of the energy an antenna concentrates in the desired direction when compared to the radiation in the other directions [13]. It can also be defined as "the ratio of the radiation intensity in a given direction from the antenna to the radiation intensity averaged over all directions" [12]. The directivity can be expressed mathematically as

$$D(\theta, \emptyset) = 4\pi \frac{U(\theta, \emptyset)}{P_{rad}} \tag{2.3}$$

And also

$$D(\theta, \emptyset) = \frac{4\pi |F(\theta, \emptyset)|^2}{\Omega_A} = D|F(\theta, \emptyset)|^2 \tag{2.4}$$

Where, the letter D represents the peak of $D(\theta, \emptyset)$.

$$\Omega_A = \iint |F(\theta, \emptyset)|^2 \, d\Omega \tag{2.5}$$

And the element of solid angle $d\Omega = \sin \theta \; d\theta \, d\emptyset$.

2.8 Gain

Gain is another important parameter describing the performance of an antenna. It is defined as the "ratio of the intensity in a given direction, to the radiation intensity that would be obtained if the power accepted by the antenna were radiated isotropically" [12]. In terms of the antenna efficiency and directivity it can be expressed as

$$G(\theta, \emptyset) = e_{cd} \, D(\theta, \emptyset) \tag{2.6}$$

Here e_{cd} is the antenna radiation efficiency.

2.9 Polarization

The polarization of an antenna is defined as the polarization of the wave transmitted by the antenna in a given direction [14]. The polarization of the electromagnetic wave is defined as the varying behavior of the electric field at any point or time. The figure traced by the vector and the sense in which the figure is traced gives us the polarization of the electromagnetic wave. This figure traced by the vector tip of the electric field is linear, circular or elliptical.

The axial ratio is normally defined as the ratio of the major axis to the minor axis of an ellipse. If the axial ratio is determined to be unity, it is circular polarization and if the axial ratio is infinity (as there is no minor axis for a straight line), the polarization is linear. All the other cases apart from these are considered to have elliptical polarization (see Figure 2.7). The extremities of elliptical polarization are the circular and linear polarization.

(a)Linear   (b)Circular   (c)Elliptical
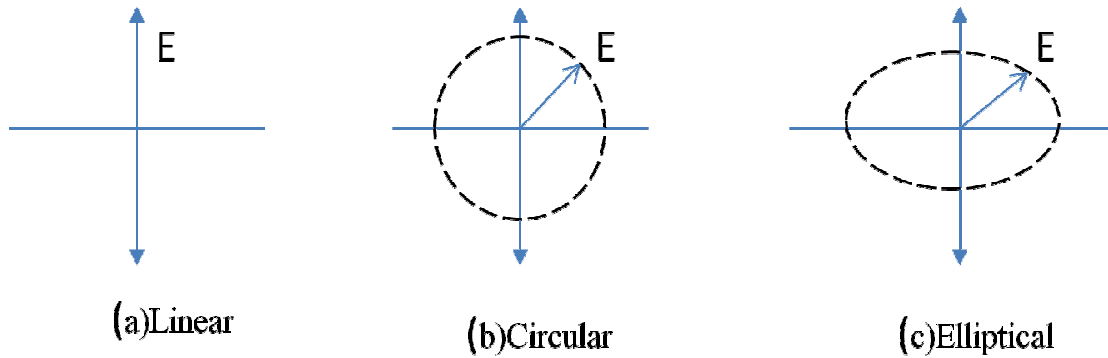
Figure 2.7: Linear, elliptical and circular polarization representation of an electromagnetic wave.

To know the sense of rotation of the E-field vector, we place a screw in the direction of propagation and rotate it in the direction of polarization. If the direction of wave propagation and screw penetration are same then it is referred to as right hand sense. Else, it is left hand sense. Consider an electrical field equation

$$\overline{E} = [E_1 \hat{x} + jE2\hat{y}]e^{-j\beta z} \tag{2.7}$$

Here, the direction of propagation is along the positive Z-axis and the direction of polarization is clockwise. If we place a screw in the direction of propagation i.e. Z-axis and rotate it in the direction of polarization (clockwise), the screw penetrates into the negative Z-direction. Thus, this is referred to as left circular polarization. The sense of rotation can be

changed in two ways. One way is by changing the direction of propagation to negative Z- axis as can be seen in (2.8), or by changing the direction of polarization to anticlockwise as seen in (2.9).

$$\overline{E} = [E_1\hat{x} + jE_2\hat{y}]\ e^{j\beta Z} \tag{2.8}$$

$$\overline{E} = [E_1\hat{x} - jE_2\hat{y}]\ e^{-j\beta Z} \tag{2.9}$$

The direction of propagation Eq(2.8) and the screw penetration are the same along the negative Z direction and are right polarized. The electric field and the direction of screw penetration are along the positive Z direction in (2.9) and are right polarized.

2.10 Pi and L matching circuits

For many antenna designs, the matching circuits are a vital part of the communication system. They are used between the feed-line and the antenna to match the antenna impedance to the feed-line impedance. This operation is necessary to efficiently couple power to and from the antenna. The L matching circuit is the simplest impedance transformation circuit as it contains just 2 reactive components. The Figure 2.8 shown below gives the general schematic diagram for L matching circuit. Like a filter, the L matching circuit also gives low pass and high pass frequency response characteristics. The L matching circuit is inherently a narrowband matching circuit.

(a)   (b)
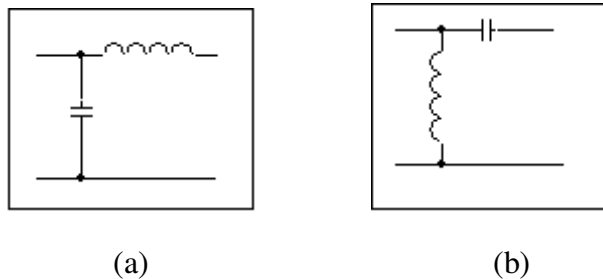
Figure 2.8: Schematic diagrams for basic L matching circuits.

A Pi matching circuit can be described as two back to back L networks. The two networks are configured as if to match the load and source to an invisible resistor at the junction [21]. The Pi matching circuit requires 3 reactive elements and gives low pass and high pass frequency response characteristics. The figure 2.9 gives the schematic diagrams for the basic Pi matching circuits. The Pi matching circuit is typically a broadband matching circuit.

<center>(a)   (b)</center>
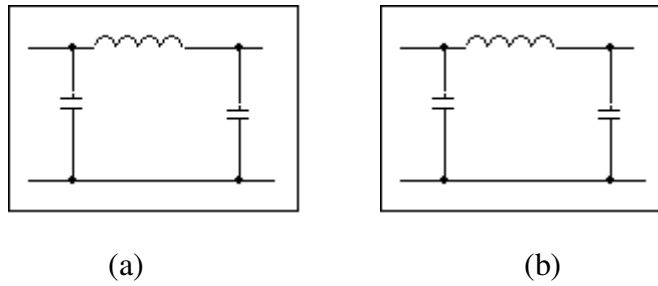
Figure 2.9: Basic Pi matching circuit schematics obtained from the combination of L circuits.

2.11 Flight Dynamics

The flight dynamics is, in general, the science of air and space vehicle orientation and the control in three dimensions. About the vehicles center of mass, there are three critical angles of rotation and are known as pitch, roll and yaw. These angles of rotation are important in this thesis study as there is a need for designing the antennas on the inflatable wings when in flight. Let the three axes shown above be the X, Y and Z axis, respectively. Let the nose tip be along the X-axis, the wings along the Y-axis and the axis along the centre of the fuselage be the Z-axis. The pitch can be described as the rotation along the Y- axis. The yaw is the rotation along the Z-axis and the roll is the rotation along the X-axis (see Figure 2.10).
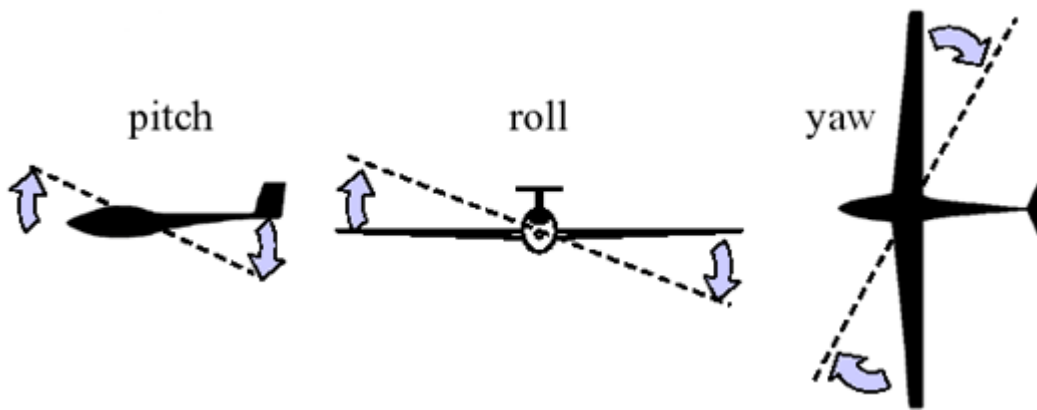
Figure 2.10: Descriptive explanation of pitch, roll and yaw, (Copyright by Toronto soaring club [15], reprinted with permission).

<center>Copyright © Rohit Reddy Tammannagari 2010</center>

CHAPTER 3- ANTENNA CONFIGURATIONS DEPLOYABLE ON INFLATABLE WINGS

3.1 Introduction

An inflatable wing is normally packed into a small volume and is opened up during flight and possibly rigidized. Being flexible, these wings also tilt during flight and this makes the antennas mounted with them flex, too. This imposes a lot of constraints on the design of antennas which are deployable on these wings. For this study, the deployable antennas for inflatable wings have the following attributes:

1. The antennas should be conformal and flexible.
2. They should be printed, painted or mounted with the wing.
3. They should be able to reach as low as VHF frequencies.
4. Antennas with high gain may be required depending on the type of application.

In addition to these requirements, the antennas are supposed to have decent radiation patterns, input impedance and gain. A set of antennas which satisfy all the above specified requirements have been designed and their description forms the crux of the sections to follow. A group of antennas which are capable of operating at the VHF, UHF and higher frequency ranges have been discussed in this chapter. A special set of branch line planar antennas operating at lower VHF range have been extensively presented in chapter 4.

3.2 Antenna configurations and their structural implementation

3.2.1 Half-wave dipole antenna

The half wave dipole is one of the simplest practical antennas and is very popular. Each arm of the antenna is one-quarter wavelength long and is fed at the center. The antenna is easy to deploy on the inflatable wing as it very simple in design and can fit anywhere. The design and the hypothetical radiation pattern for a dipole are as shown in Figure 3.1. The Figure below also shows the inflatable wing with which the dipole is mounted. When a dipole is half-wavelength long, or a bit less, the input reactance tends to be zero. Thus, input impedance is essentially equal to the radiation resistance. The dipole has a radiation resistance of around 70Ω.

<center>(a)   (b)</center>
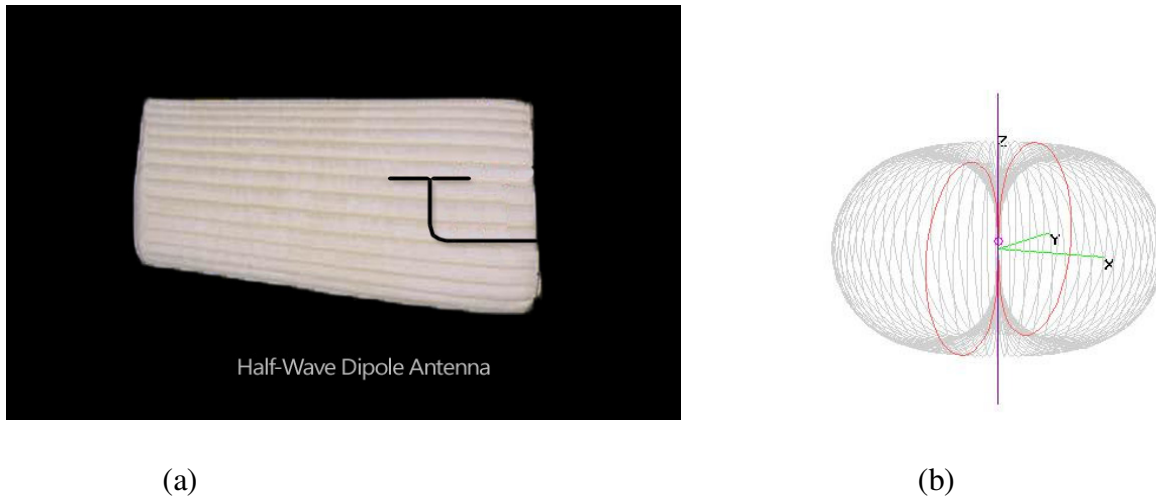
<center>Figure 3.1: Half-wave Dipole antenna (a) A dipole antenna on an inflatable wing (b)
Hypothetical radiation pattern of a dipole antenna.</center>

The dipole can be made with flexible materials, like coaxial cables, and mounted with the inflatable wing. For the purpose of design, the frequency has been selected to be 900 MHz as this falls in the radio frequency range. The frequency of operation for antennas designed in the Big Blue project was also 900 MHz and that is also one of the reason this value has been selected. Thus, the length of the dipole comes out to be 0.166 meters thereby, making the length of each arm to be 0.083 meters. The dipole can be deployed anywhere on the wing. The dipole can be constructed using coaxial cables or thin wires and can be just integrated along the spars of the wing as shown in the Figure 3.1. The length of the wing that was used for this thesis was 0.889m. Thus, the lower limit for the frequency of operation is 168MHz for the half-wave dipole. The simulation results for a Half-wave dipole antenna have been presented in detail in chapter 5.

3.2.2 Yagi-Uda Antenna

A Yagi-Uda antenna is another practical and popular radiator available to us. A Yagi antenna is a parasitic array of dipoles as can be seen structurally integrated along with the inflatable wing in Figure 3.2. This antenna consists of a driven element, which is the element connected to the transmission line. This driven element is generally a dipole. The parasitic elements are referred to as directors and the one on the right acts as a reflector. The currents on these parasitic elements are induced by mutual coupling. The Yagi antennas have an end-fire radiation pattern as can be seen from the hypothetical radiation pattern presented in Figure 3.3. The end-fire pattern is achieved by keeping the length of the directive elements a bit smaller than that of the driven element. The reflector is normally a bit longer than the driven element. In general, the length of the driven element is slightly less than $\lambda/2(0.45-0.49\lambda)$ and the directors are in the range of $0.4-0.45\lambda$. All the directors are not necessarily of the same length
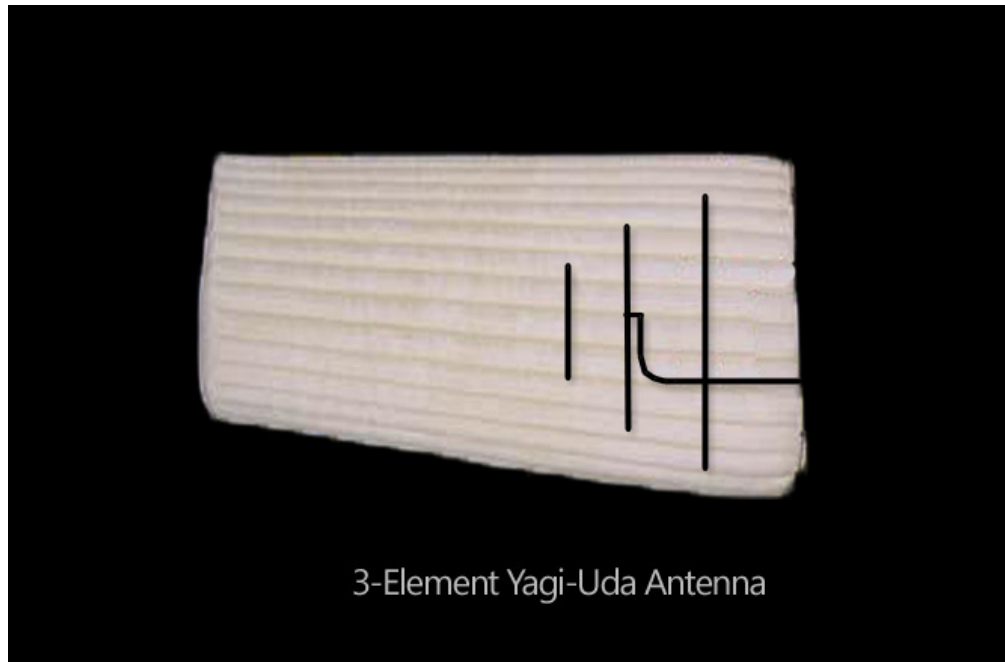
<center>23</center>
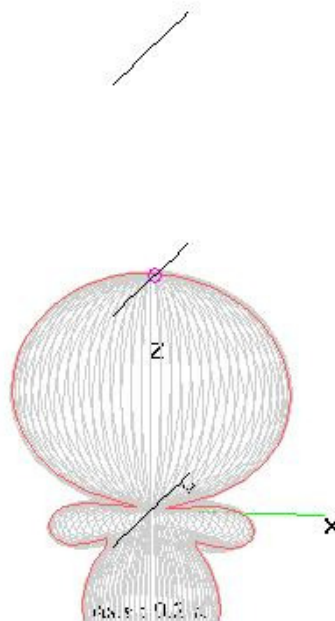
Figure 3.2: Configuration of a Yagi-Uda antenna.

Figure 3.3: Radiation pattern (a) A 3-element Yagi antenna (b) H-plane pattern (c) E-plane pattern.

and diameter. The spacing between the elements is not necessarily uniform in all the conditions. The impedance of the directors is capacitive with the current leading the induced emf and the reflector is inductive in nature with the current lagging the induced emf in phase. Thus, properly spaced elements with lengths slightly less than the resonant length ($\lambda/2$) act as directors. On the same grounds, properly spaced elements with lengths equal to or greater than resonant length act as reflectors [12]. In practice, the first element of the Yagi acts as the reflector. Addition of more reflectors adds very little to the overall performance of the antenna and thus is normally not done. However, the addition of the directive elements leads to considerable performance enhancements. There is a limit to the number of elements that can be added to the antenna array as, after a point addition of further elements does not bring much improvement in the performance due to progressive reduction in the magnitude of the induced currents. The Yagi antennas are lightweight, easy to build, low cost and provide desirable characteristics [12]. This is the reason they are very widely used. Figure 3.4 below shows a pair of Yagi-Uda antennas on the FPAT building of University of Kentucky. The pair of Yagi's are:

- 21-element Yagi (2m range) on the left and
- 42-element Yagi (70cm range) on the right.

Figure 3.4: A pair of Yagi-Uda antennas at the University of Kentucky used for satellite and amateur-radio communication.

The Yagi antenna can be placed anywhere along the length of the wing, preferably near the fuselage for easy feed access to the driven element of the antenna. A three element Yagi has been designed for the inflatable wing available and the frequency of operation is set to be 900MHz for the purpose of design as this falls in the radio frequency range and the same frequency of operation was used in the Big Blue project. The lengths of the elements came out to be 0.1596, 0.151 and 0.1503 meters for the reflector, driver and the director respectively. The spacing

between the elements was uniform and around 0.0833 meters. The Yagi antenna can be constructed using coaxial cable, thin wires or can be printed onto the wing and can be integrated along the spars of the wing as shown in Figure 3.2. The length of the wing that was used for this thesis was 0.889 meters. The maximum number of directors that can be used for this length is 8. The lower limit for the frequency of operation is similar to that for the half-wave dipole. The lower limit is 168MHz when the elements are as shown in Figure 3.2 and width of the wing is set to the width of length of the reflector. The simulation results for three, four and five element Yagi-Uda antenna have been presented in detail in chapter 5. As we go beyond four elements there is not much improvement in the antenna parameters.

3.2.3 Bow-tie antenna

The Bow-tie antenna and the set of antennas presented in the following sections have come into picture only because their shape allows them to be easily deployable with the wings for the UAV's. The Bow-tie antenna is a broadband design used in a lot of communication applications. These antennas can be printed on rectangular substrates and used in wireless applications. The Bow-tie as mounted for the wing of a UAV is shown below in Figure 3.5 and the radiation pattern of a Bow-tie antenna is given in Figure 3.6.

Bow-tie Antenna

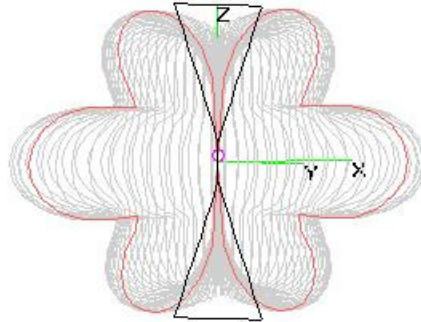Figure 3.5: A Bow-tie antenna as mounted with a wing for UAV.

Figure 3.6: Radiation pattern of a Bow-tie antenna.

There are no set guidelines to obtain the dimensions. Thus, a lot of different dimensions were tried and the antenna properties noted for each set of dimensions, leading to a good set of values for the dimensions. When the base of the triangle is of the order of λ/2 and the median of each triangle is λ/2, acceptable radiation pattern and impedance data are obtained. The Bow-tie is fed at the center of the line intersecting the two triangles. The Bow-tie can be constructed using coaxial cable, thin wires, and flexible substrates with good dielectric properties and can also be printed onto the wing and integrated along the spars of the wing as shown in Figure 3.5. The length and breadth of the wing that was used for this thesis was 0.889 meters and .3048 (shorter wing tip) meters respectively. The lower limit for the frequency of operation is 492MHz. A Bow-tie antenna was designed according to the design constraints set by the wing dimensions for a frequency of 492MHz. This frequency of operation was chosen because the Bow-tie gives good radiation pattern and gains at this frequency. Also, this value falls in the radio frequency range. The simulation results for the Bow-tie antenna have been presented in detail in chapter 5.

3.2.4 Linear Tapered-slot antenna

A Linear Tapered- slot antenna looks off the wingtip. For the purpose of design the linear version of this antenna has been considered. This antenna can be mounted with a wing as shown in Figure 3.7.The center of the line joining the two tapering slots has been considered as origin. The frequency of operation for the design constraints posed by the dimensions of the wing was 370.5MHz. The Tapered-slot antenna gives good gain and radiation patterns at this frequency. Moreover, this value of frequency lies in the radio frequency range. Like the Bow-tie antenna, there are no proper guidelines for determining the dimensions of the Tapered-slot antenna. For

obtaining a proper radiation pattern and characteristics, several empirical measurements were evaluated. When the base length was set to λ/2 and each vertical side to λ, optimum results were obtained. The Tapered-slot antenna can be constructed using coaxial cable, thin wires, and flexible substrates with good dielectric properties. The Tapered-slot antenna can also be printed onto the wing and integrated along the spars of the wing as shown in Figure 3.7. The length and breadth of the wing that was used for this thesis was 0.889 meters and .445 meters (width of the broader wing tip) respectively. The lower limit for the frequency of operation is 337MHz. The simulation results for the Tapered-slot antenna have been presented in detail in chapter 5.
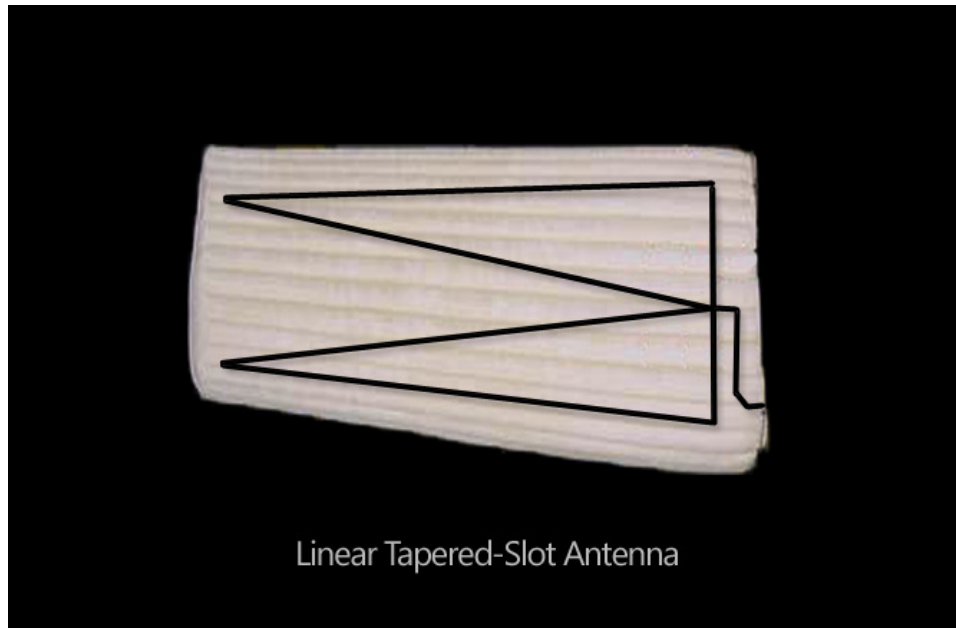
Figure 3.7: A Tapered slot antenna mounted with a wing of a UAV.

3.2.5 Maltese-cross antenna

The Maltese-cross is an antenna that can be deployed with the wing of an inflatable wing. However unlike the Bow-tie and the Tapered slot antenna discussed in previous sections, this antenna cannot make use of the entire length of the wing [16]. It can receive horizontal, vertical and circular polarization. This antenna is commonly used with GPS satellite and DCS 1800 personal communication systems [17]. A Maltese antenna mounted with a wing is shown in Figure 3.8.

Figure 3.8: A Maltese-cross antenna mounted with a wing.

The Maltese-antenna is circularly polarized. The two bi-cones constituting the Maltese were placed on the top and bottom of the inflatable wing. Both these bi-cones are fed at the centers of the lines intersecting the two set of triangles. The thickness of the wing separates the two bi-cones of the Maltese and this thickness has been set to $\lambda/4$ to obtain an excitation of 90 degrees between the two bi-cones and thereby, achieving circular polarization. As has been the case in the above sections there are no clear guidelines on what the dimensions should be and thus a set of values were put in to observe the antenna parameters. The best fit came up when the base on each side was set to the $\lambda/2$ and the height of the bi-cone to λ. Fabricated Maltese used for the GPS and DCS 1800 applications is shown below in Figure 3.9. The frequency of operation for the design has been set to 1973MHz based on the design constraint set by the thickness of the wing as explained above. The Maltese gives good radiation pattern and gains at this frequency. Also, this value of frequency falls in the radio frequency range and the dimensions have been calculated for this value of frequency.
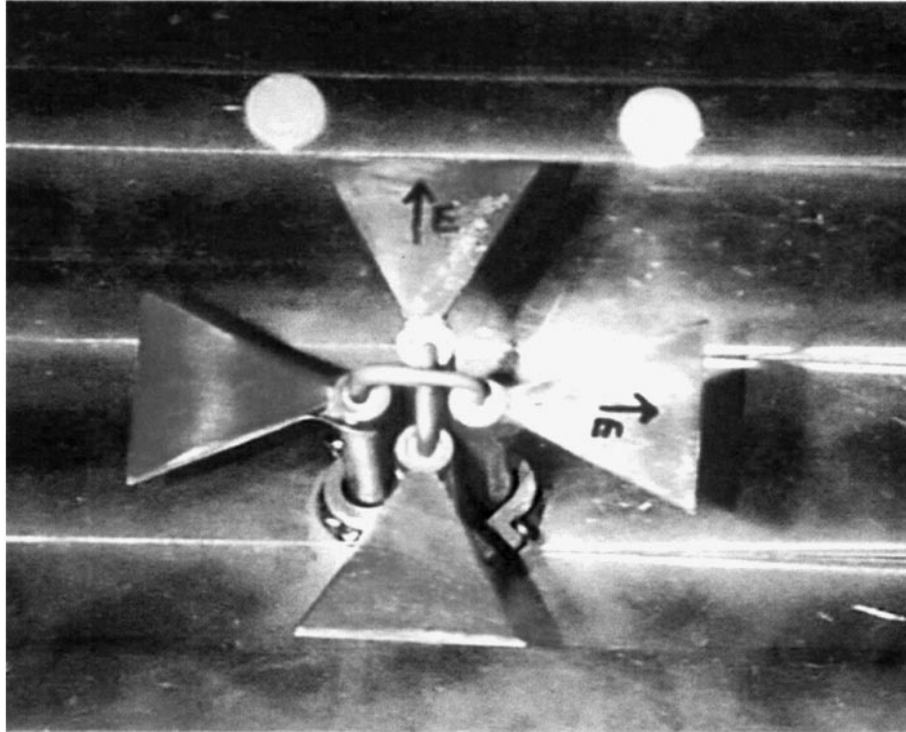
Figure 3.9: A Maltese-cross antenna attached to cylindrical baluns, (Copyright by © 2003IEEE [17], reprinted with permission).

The Maltese-cross antenna can be constructed using coaxial cable, thin wires, and flexible substrates with good dielectric properties. They can also be printed onto the wing and integrated along its spars as shown in Figure 3.9. The length and breadth of the wing that has been used for this thesis is 0.889 meters and .3048 (shorter wing tip) meters respectively. The lower limit for the frequency of operation is 984MHz. The simulation results for the Maltese-cross antenna have been presented in detail in chapter 5.

3.3 Conclusions

This chapter has dealt with various sets of antennas focused mainly to operate at the VHF and the UHF range. The set of requirements pointed out in the first section, such as flexibility, conformability, and high gain are achieved using these antennas. The configurations, dimensions and the positions of all the antennas on the inflatable wing have been thoroughly discussed. In addition to these, the theoretical radiation patterns and some real world applications of these antennas have also been presented.

CHAPTER 4- BRANCH LINE PLANAR ANTENNA

4.1 Introduction

Branch line planar antennas are also sometimes referred to as serpentine antennas. The dipole design that is being presented in this chapter is based on branch line planar monopole design. Because of its serpentine shape, this class of antenna can be incorporated along the length and breadth of an inflatable wing. The idea here is to make use of the structure of the wing and mould the antenna accordingly. These relatively complex antennas have the frequency of operation in the lower VHF range. This chapter covers various modules of branch line planar antennas that can be mounted with an inflatable wing. In addition to that, the structural implementations and the dimensions of this class of antennas have also been discussed. The guidelines on the spacing between elements have also been examined. They can be deployed with the inflatable wings by running the flexible coaxial cables along the spars or they can be printed on a flexible substrate like FR4 (thickness 0.8mm and relative permittivity 4.4) [18]. The antenna characteristics and comparison of results of all the antennas discussed in previous chapters and this chapter are presented in Chapter 5.There are, and can be, several applications of branch line planar antennas because of their shape and frequency of operation. Some of them are

1. They are used in place of traditional monopoles as their usage reduces the size of mobiles phones.
2. These can be used on an inflatable wing for communication as its design can be modified according to the structure of the wing.
3. They can be used for long distance radio communication at lower frequency as these antennas operate between 30-50MHz. There are not many efficient antennas, given the wing size restriction, in the lower VHF range and this application to inflatable wings is a first.

4.2 Structural Implementation

There are two different ways in which the branch line planar antennas have been structurally mounted with an inflatable wing. The designs are for an inflatable wing used for the Big Blue project, having a length of 0.889 meters and a breadth of 0.445 meters. This wing has 13 inflatable spars along its length. The available wing has been shown structurally integrated with the branch line planar antennas in Figures 4.1 and 4.2 below. The complete structure of the wing is used by running the antenna along the length and breadth of the spars (the structural or skeletal support system of a wing). The antennas presented here have been specifically designed for an inflatable wing which has only horizontal spar support. The first module has the serpentine lines propagating along the length of the wing as shown in Figure 4.1:
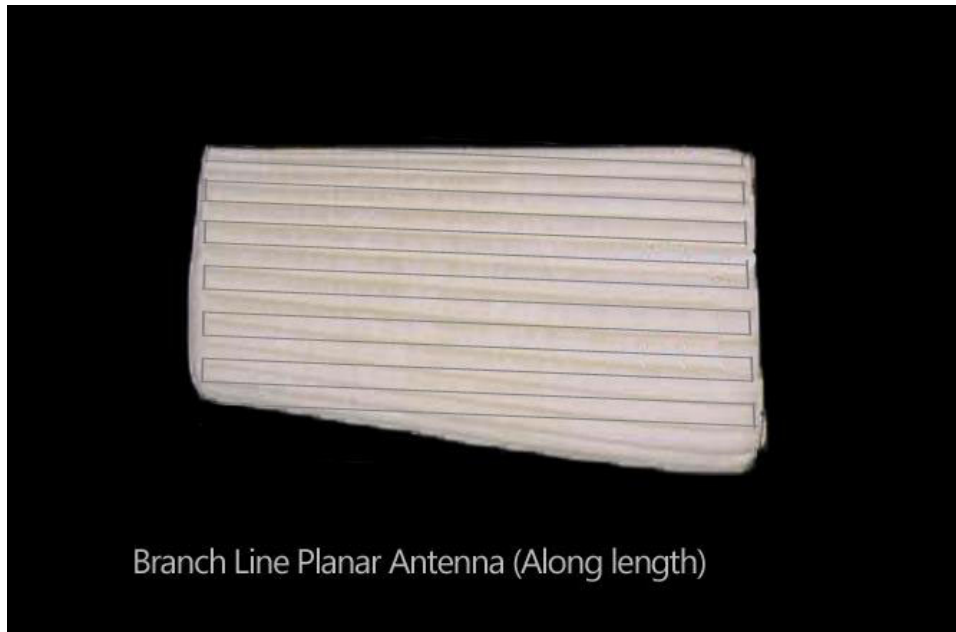
Figure 4.1: Branch line planar antenna (along length).

This design is pretty simple as the antenna just runs along the length of the spars of the wing. The second module has the serpentine lines propagating along the width of the wing as shown in Figure 4.2:
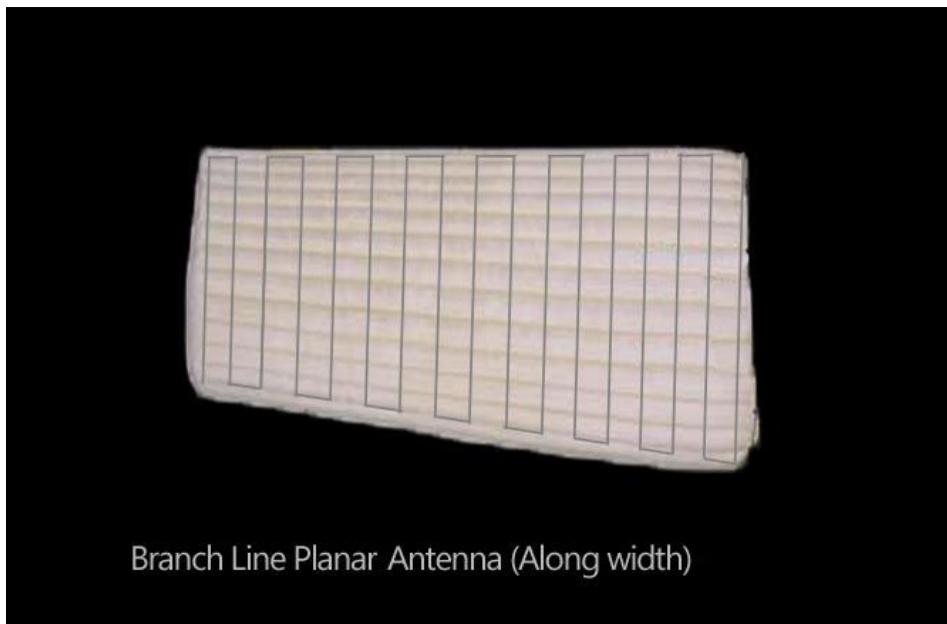

Figure 4.2: Branch line planar antenna (along width).

For determining the optimum spacing between elements, varying lengths have been used and the results considered. For the branch line planar antenna along the width a spacing of L/6 (L

being the length of each element along the width of the wing) gave acceptable electrical properties for this antenna structure.

4.3 Branch line planar antenna (along length)

The inflatable wing used here has thirteen spars. Thus, there are thirteen elements along the length and twelve connecting elements along the width respectively. As the spacing between the elements along the length is nothing but the spacing between the spars, it is preset and the antenna was designed using this spacing due to its mechanical convenience. The dimension of the elements is the same as the dimension of the spars and the total length of the antenna adds up to 11.898 m. The dimensions of the various elements of the antenna have been measured and are presented in Figure 4.3:
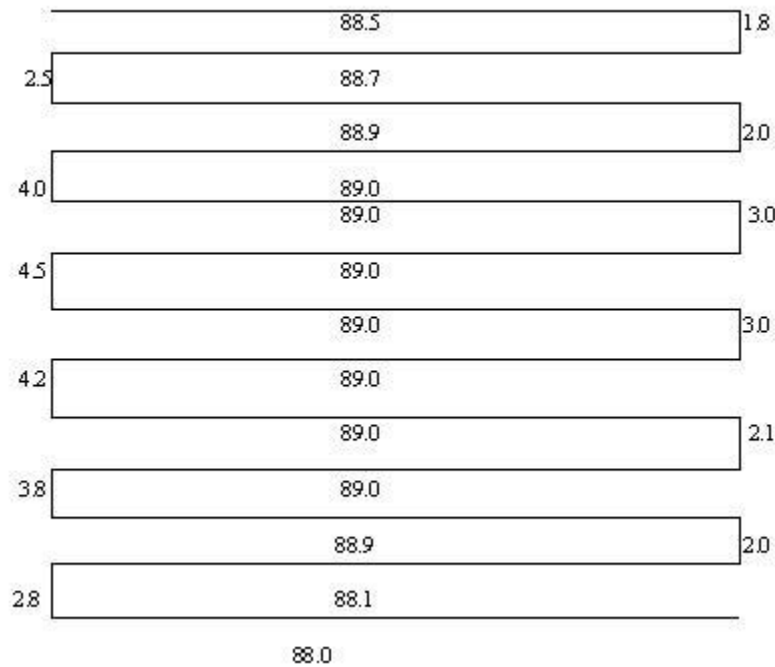

Figure 4.3: Measured dimensions of individual elements (in cm).

This dipole antenna is fed at the midpoint. Considering the length of the antenna as the length of a half wave dipole yields the theoretical frequency of operation as 12.607 MHz. However, the impedance becomes resonant only at 38.1484 MHz. This difference in frequencies is due to the coupling effects between adjacent sections of the antenna.

4.4 Branch line planar antenna (along width)

The number of elements along the width varies according to the spacing between them. As the spacing here is not preset by the wing structure a number of spacing combinations were evaluated. Eventually, a spacing of L/6 produced desired results. Other dimensions used were not able to provide a decent radiation pattern, gain, VSWR, and input impedance. A spacing of L/6 gave a well directed radiation pattern, gain and VSWR. The input impedance obtained was a little low but was brought to 50Ω by using optimization and matching techniques. For L/6 spacing, there are seventeen elements along the width of the wing and the length of each element is 0.307 m. From the computational formula provided above, the spacing between the elements came down to 0.05116 m. The total length of the antenna was 6.035 m. The dimensions of the individual elements obtained using the above guidelines are shown in Figure 4.4:
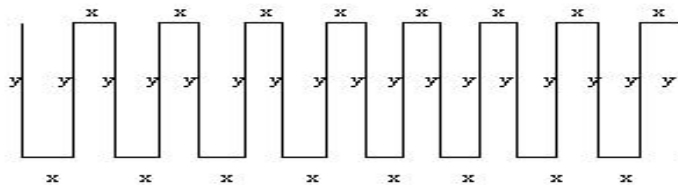
x=5.116 cm, y= 30.7cm
Fig 4.4: Dimensions of individual elements (in cm).

The antenna has been designed as a half wave dipole and fed at the midpoint of the antenna. As explained in the previous design because of the coupling between adjacent sections, the impedance was resonant at 44.93 MHz as opposed to theoretical frequency of 12.4275 MHz

4.5 Conclusions

The idea of using the structure of the inflatable wing to design an antenna was realized in the form of branch line planar antennas. These antennas not only mount with the wing structure, but also give desirable characteristics which are essential for transmission and reception of signals during flight. Two different modules of branch line planar dipoles were presented and designed. In addition to these aspects, the guidelines for spacing between elements of the antenna and the effects of coupling on frequency of operation have also been described. Thus, the motive of designing an antenna which can operate in the low VHF range has been met.

CHAPTER 5- RESULTS AND EVALUATION

5.1 Introduction

The simulation results for all the antennas discussed in Chapters 3 and 4 are presented in this Chapter. The antenna modeling was achieved with the help of two programs, namely Wirecode and 4NEC2 (4NEC2- Numerical Electromagnetics Code). These programs are based on the method of moments and are briefly discussed here. A comparison of the various antenna configurations based on antenna parameters has also been presented.

5.2 Program overview

5.2.1 Wirecode

One of the software programs that was used to design the antennas for this thesis is known as Wirecode [14]. This program was written by Dr. William A. Davis from the Virginia Polytechnic Institute and State University. This code uses the method of moments and is based on MININEC. It was written in Turbo Pascal. The Wirecode models the antennas as thin wires. The user has to model antenna as piecewise straight wire elements and give the co-ordinates of each end of the wire as an input along with the number of segments into which each wire is divided. The user also has to give proper connection between the wires and can select the point of the feed and frequency of operation accordingly. The onus here is to make the input impedance near resonant as this makes matching the antenna to a transmission line straightforward. Adjustments pertaining to the length and frequencies can be made to obtain desired results. The Wirecode provides us with the voltage, current, impedance, total power, pattern data and current distribution plots [14]. The Wirecode program was primarily used to verify the results obtained using 4NEC2 (see section below).

5.2.2 4NEC2

4NEC2[19] is a windows based tool for creating, viewing, optimizing, matching and checking 2D and 3D antenna geometry structures and to generate and display near/far-field radiation patterns. Also the current distribution along the antenna geometry can be obtained. It is also based on the method of moments and models antennas as thin wires like the Wirecode. Linear or logarithmic SWR, F/B ratio and impedance line-charts can also be obtained using this program. The antenna geometry can be created or edited with the help of a 4NEC2 editor or a geometric editor according to the convenience of the user. With the included optimizer the antenna variables can be optimized for gain, resonance, SWR, efficiency and/or F/B ratio. The included RLC matching capability provides for L, pi, and T networks for low-pass and high-pass matching. The simulated results for each antenna are provided in the sections below.

5.3 Half-wave dipole antenna

The half-wave dipole is assumed to be oriented along the Z-axis. In the notepad editor, which is used for providing the antenna dimensions in 4NEC2, the dipole has been divided into 2 wires each consisting of 10 segments. The antenna profile as obtained from a 4NEC2 snapshot is as shown in Figure 5.1.
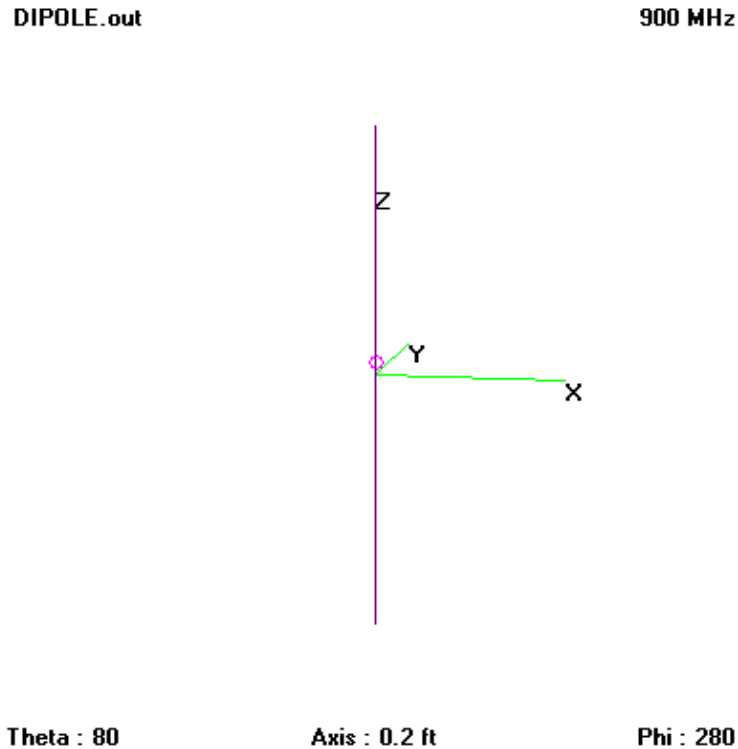

Figure 5.1: A Half-wave dipole antenna profile.

The dipole has been fed at the center where the current is at a maximum and provides a low impedance feed point which is straightforward to match. A screenshot of the 4NEC2 window reflecting the various antenna parameters is as shown in Figure 5.2. As can be seen from Figure 5.2 the frequency of operation has been set to 900MHz as this falls in the radio frequency range. The frequency of operation for antennas designed in the Big Blue project was also 900 MHz and that is also one of the reason this value has been selected. A pi- matching circuit was used. The antenna is designed as if in free space. This is acceptable as the fabric and the inflatable wing structure approaches free space characteristic parametersϵ_0, μ_0. The radiation pattern for the half-wave dipole as obtained using 4NEC2 is presented in the Figures 5.3 and 5.4. As can be seen from Figure 5.4, the radiation pattern for a dipole is in the form of a doughnut. The antenna has Omni-directional. The rectangular plot for a dipole is shown in Figure 5.5 and the maximum gain obtained from this plot is approximately 2.1dBi. This value of gain is typical for a half- wave dipole antenna. The current distribution along a dipole is roughly sinusoidal. It falls to zero at the

end and is at a maximum in the middle. Conversely the voltage is low at the middle and rises to a maximum at the ends. The current distribution along a half-wave dipole is shown below in Figure 5.6.
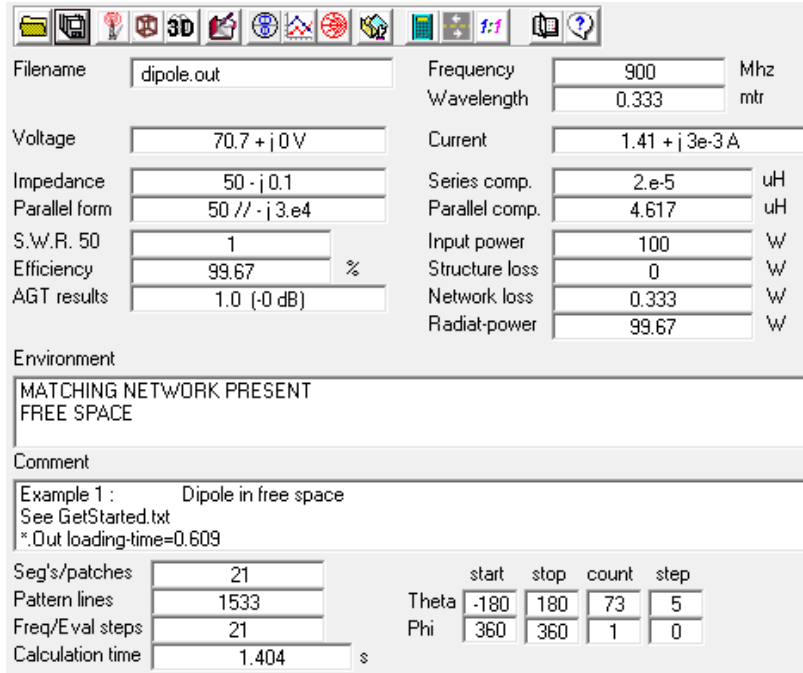

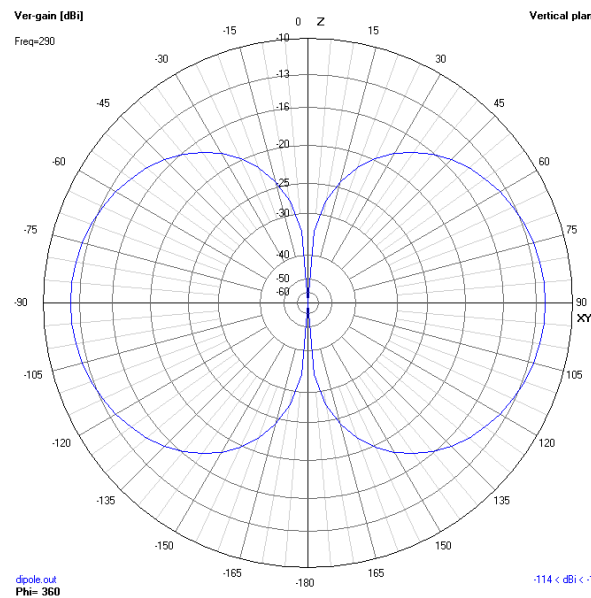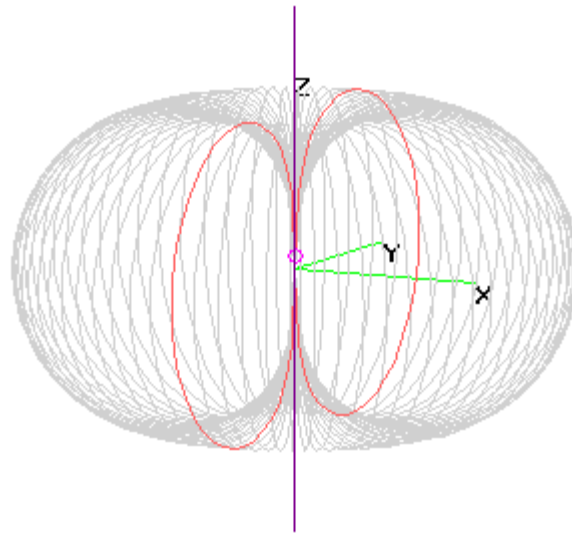Figure 5.2: 4NEC2 screenshot reflecting antenna parameters.

Figure 5.3: Radiation pattern for a Half-wave dipole antenna.

37

Theta : 81   Axis : 0.2 ft   Phi : 296

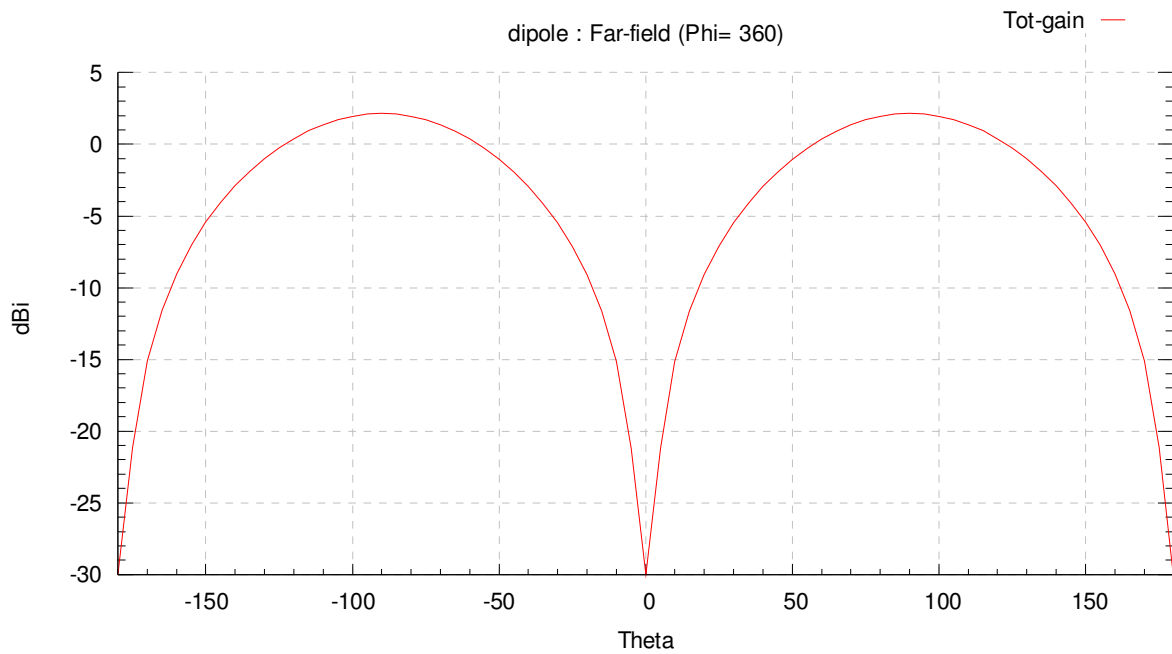Figure 5.4: A superimposed antenna cum radiation pattern plot.

dipole : Far-field (Phi= 360)   Tot-gain ——

Figure 5.5: Rectangular plot of a Half- wave dipole.
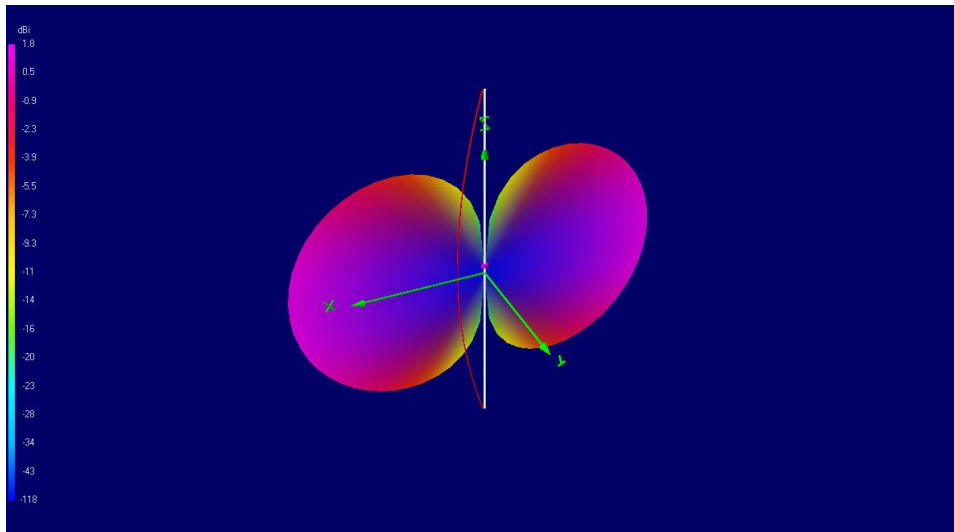
Figure 5.6: Current Distribution for a Half-wave dipole antenna.

5.4 Yagi-Uda antenna
5.4.1 Three-element Yagi-Uda antenna

The three-element Yagi-Uda antenna is assumed to be oriented along the Z-axis with Y-directed elements. In the notepad editor, which is used for providing the antenna dimensions in 4NEC2, the Yagi antenna has been divided into 4 wires each consisting of 10 segments. The antenna profile as obtained from a 4NEC2 snapshot is as shown in Figure 5.7.
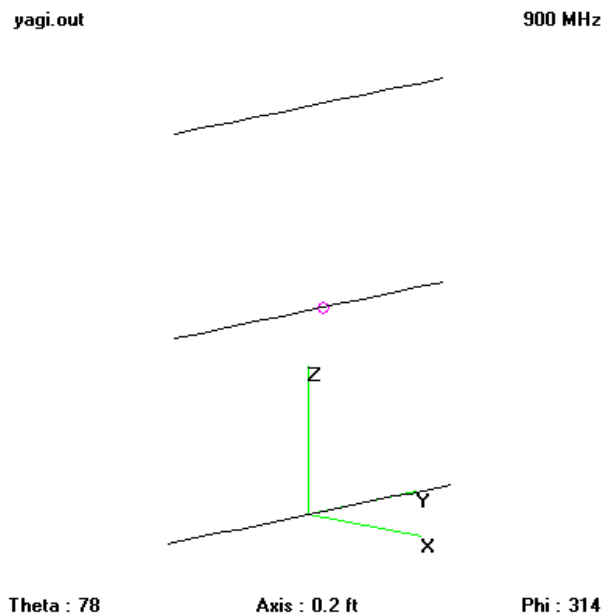

Figure 5.7: Antenna profile of a three-element Yagi-Uda antenna.

The Yagi has been fed at the center of the driver element where the current is at a maximum and provides a low impedance feed point which is straightforward to match. A screenshot of the 4NEC2 window reflecting the various antenna parameters is as shown in Figure 5.8. As can be seen from the Figure 5.8, the frequency of operation has been set to 900MHz as this falls in the radio frequency range and the same frequency of operation was used in the Big Blue project. A pi matching circuit was used. The antenna is modeled using free space conditions. The radiation pattern for the three-element Yagi as obtained using 4NEC2 is presented in Figures 5.9 and 5.10 below. As can be seen from Figure 5.10 the radiation pattern for a Yagi is an endfire pattern. The rectangular plot for the Yagi antenna is shown in Figure 5.11 and the maximum gain obtained from this plot is approximately 8.5 dBi. Current distributions along Yagi elements are similar to that for a half-wave dipole and are roughly sinusoidal. The current distribution along a three-element Yagi is shown below in Figure 5.12. The addition of directors often leads to a higher gain. The parameters for the four and five element Yagi antennas have been presented in the sections to follow. For the wing dimensions, a maximum of 8 directors can be used.
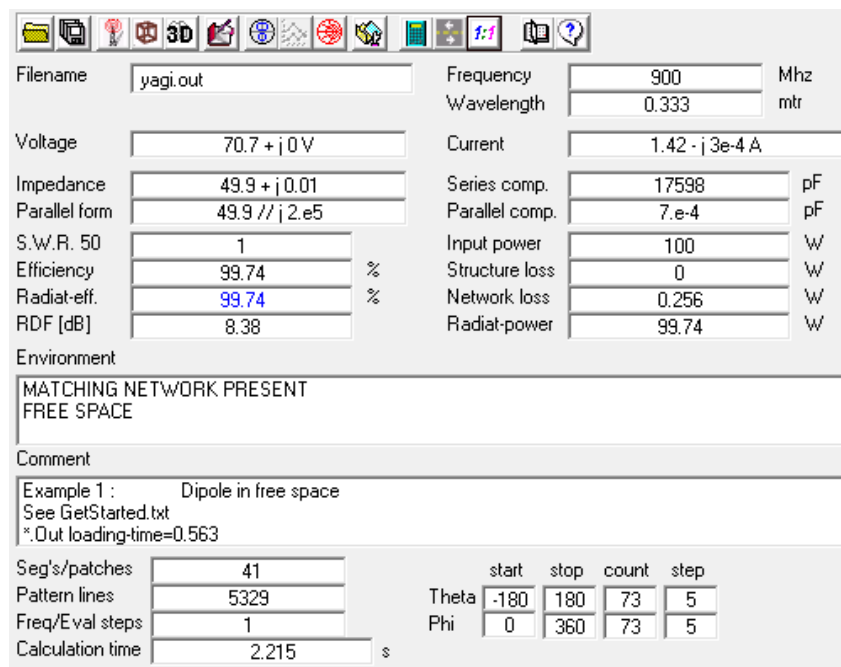

Figure 5.8: 4NEC2 screenshot reflecting antenna parameters for a three-element Yagi.
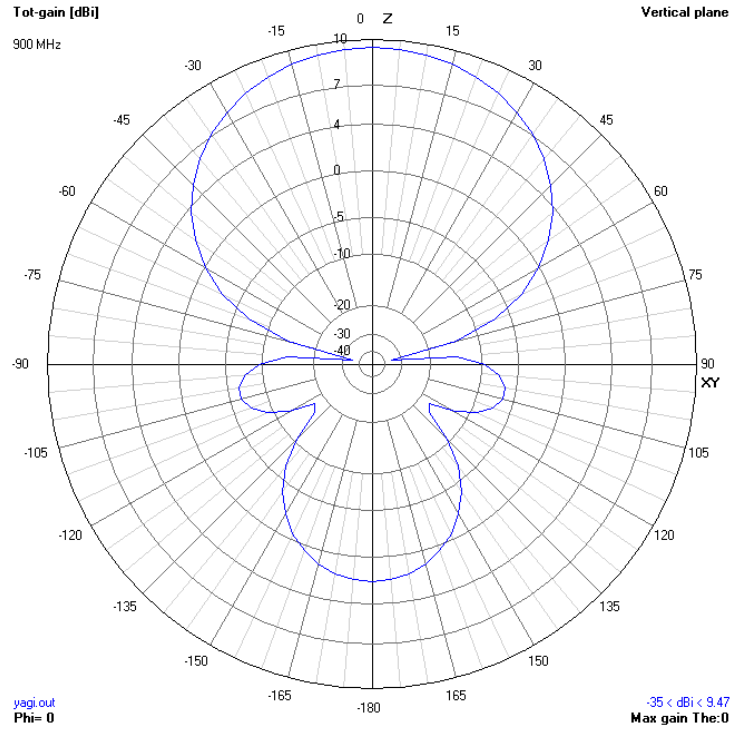
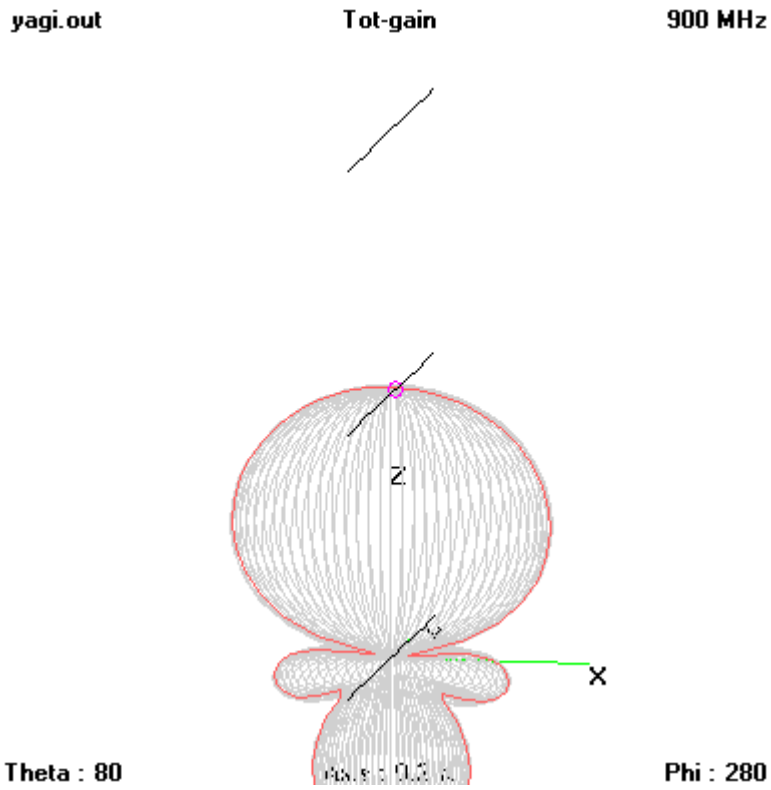Figure 5.9: Radiation pattern for a three-element Yagi antenna.

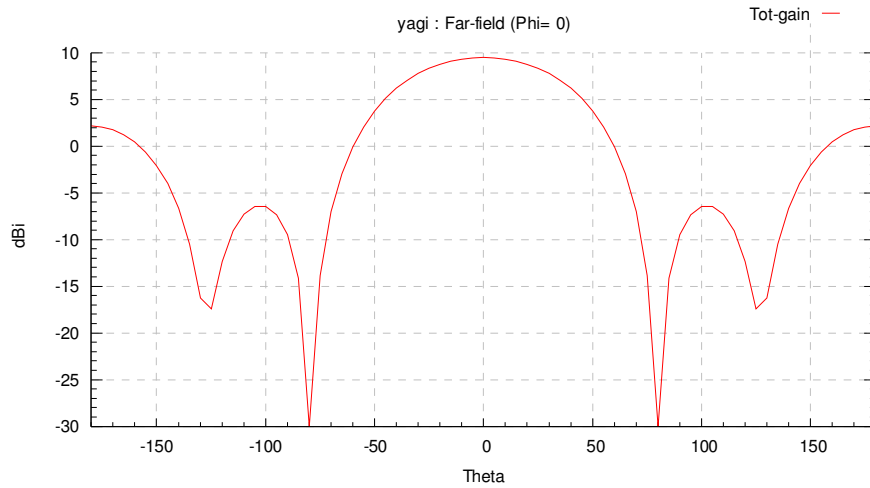Figure 5.10: A superimposed antenna/radiation pattern plot.

41

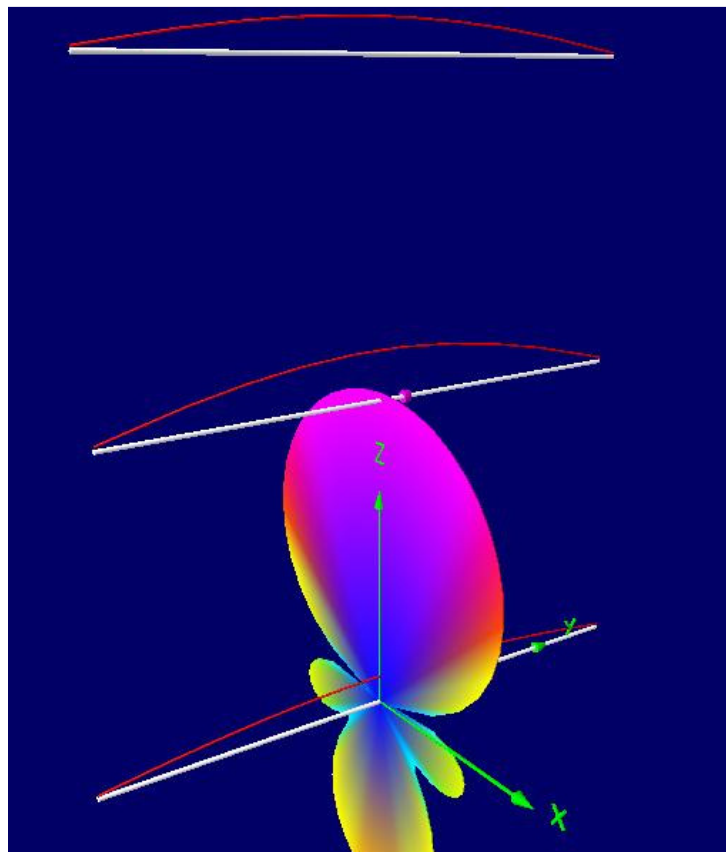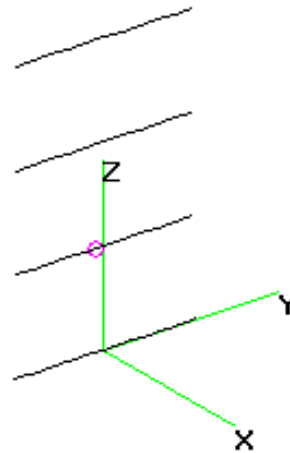Figure 5.11: Rectangular plot of a three-element Yagi antenna.

Figure 5.12: Current Distribution for a three-element Yagi antenna.

5.4.2 Four-element Yagi-Uda antenna

The antenna profile for a 4-element Yagi is as shown in Figure 5.13.

yagi4.out   900 MHz

Theta : 63   Axis : 0.5 ft   Phi : 323

Figure 5.13: Antenna profile of a four-element Yagi-Uda antenna.

The four-element Yagi has an input impedance of 60.7Ω (real part) as opposed to 41.4Ω for a three-element Yagi. The radiation pattern for this four-element Yagi is as shown in Figure 5.14. As can be observed from the Figure, there is an increase in the gain over the 3-element Yagi.
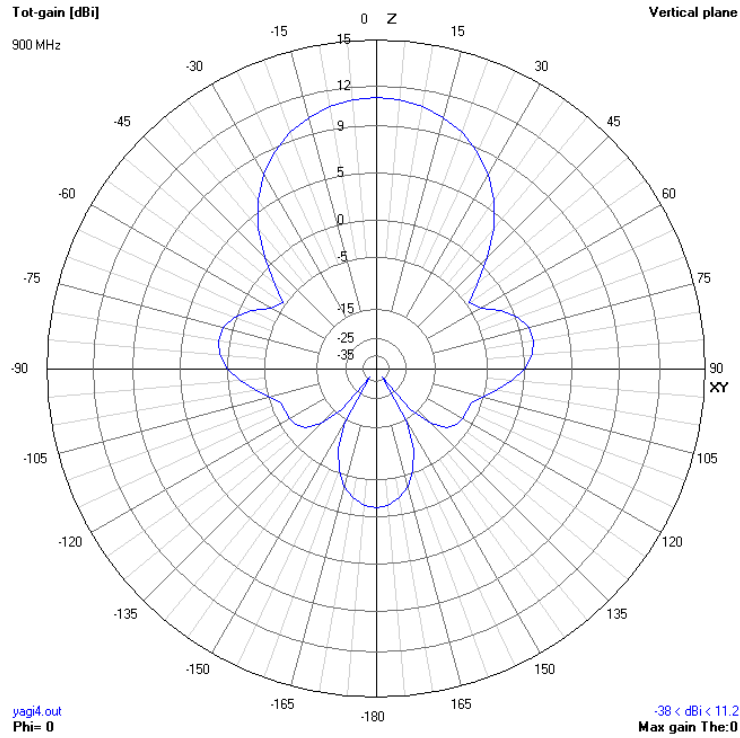
Figure 5.14: Radiation pattern for a four-element Yagi antenna.

5.4.3 Five-element Yagi-Uda antenna

The profile of a 5-element Yagi antenna is as shown in Figure 5.15.
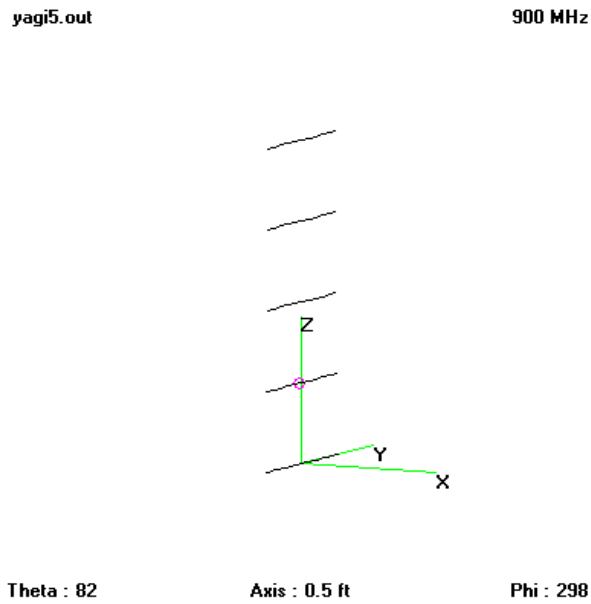

Figure 5.15: Antenna profile of a five-element Yagi-Uda antenna.

The five-element Yagi has an input impedance of 44.8Ω (real part) as opposed to 41.4Ω for a three-element Yagi. The radiation pattern for this five-element Yagi is as shown in Figure 5.16. The addition of the extra element did not lead to a noticeable increase in gain when compared to a four-element Yagi. Thus, the benefit of adding the extra director for this design is not justified.
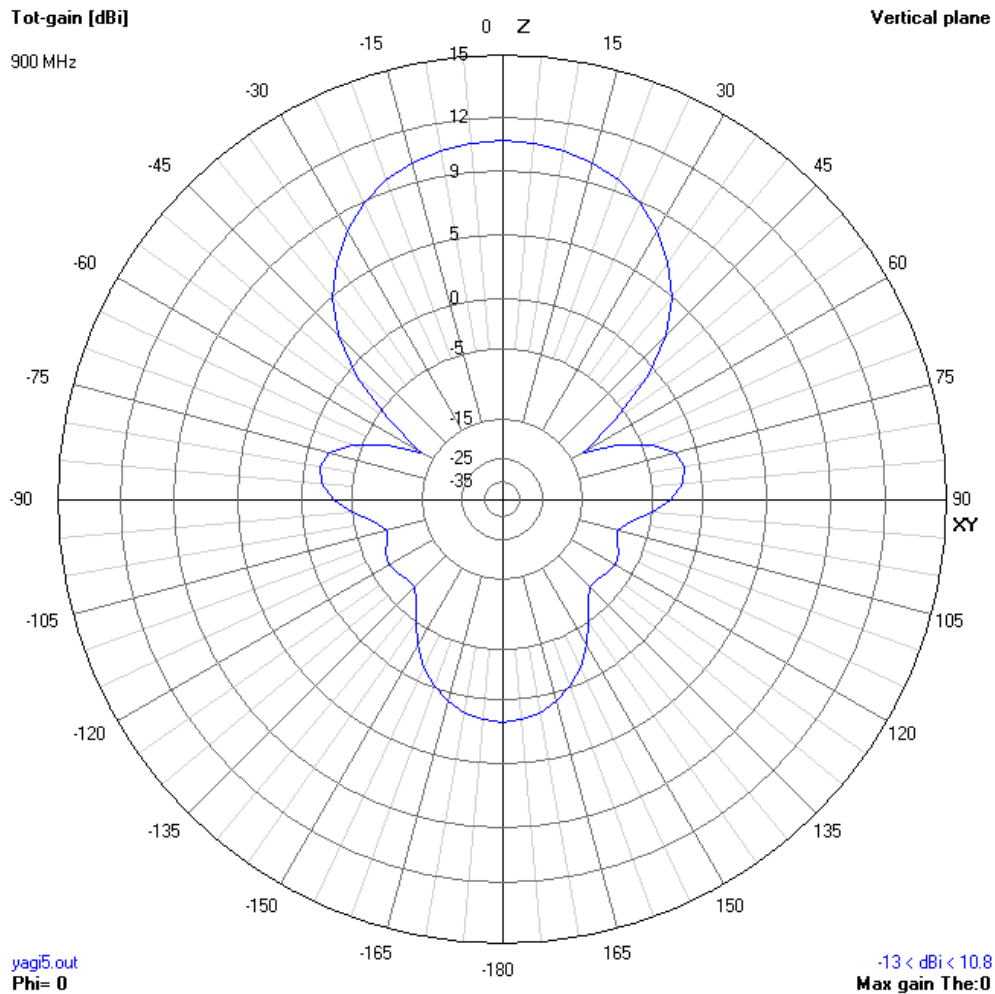

Figure 5.16: Radiation pattern for a five-element Yagi antenna.

5.5 Bow-tie antenna

The Bow-tie antenna has been oriented along the Z-axis. In the notepad editor, which is used for providing the antenna dimensions in 4NEC2, the bow-tie antenna has been divided into 7 wires each consisting of 10 segments. The antenna profile as obtained from a 4NEC2 snapshot is as shown in Figure 5.17.
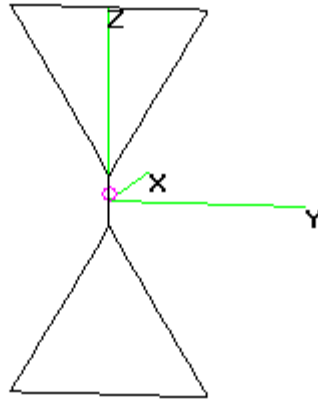
Figure 5.17: A Bow-tie antenna profile.

The antenna has been fed at the center of the line intersecting the two triangles. A screenshot of the 4NEC2 window reflecting these mentioned parameters is shown in Figure 5.18. The frequency of operation for the dimensions given in Chapter 3 is 492MHz.The Bow-tie gives good radiation pattern, and gains at this frequency. Also, this frequency falls in the radio frequency range. The antenna is modeled as if in free space and a pi- matching circuit was used. The radiation pattern for the bow-tie as obtained using 4NEC2 is presented in the figures 5.19 and 5.20 below. The radiation pattern has many side lobes and the bow-tie offers a maximum gain of 7.13 dBi (see Figure 5.21). The current distribution along a bow-tie antenna is shown below in Figure 5.22. The bow-tie uses the wing structure better than the dipole or Yagi antenna and was placed along the length of the wing.

Figure 5.18: Antenna parameters for Bow-tie antenna.

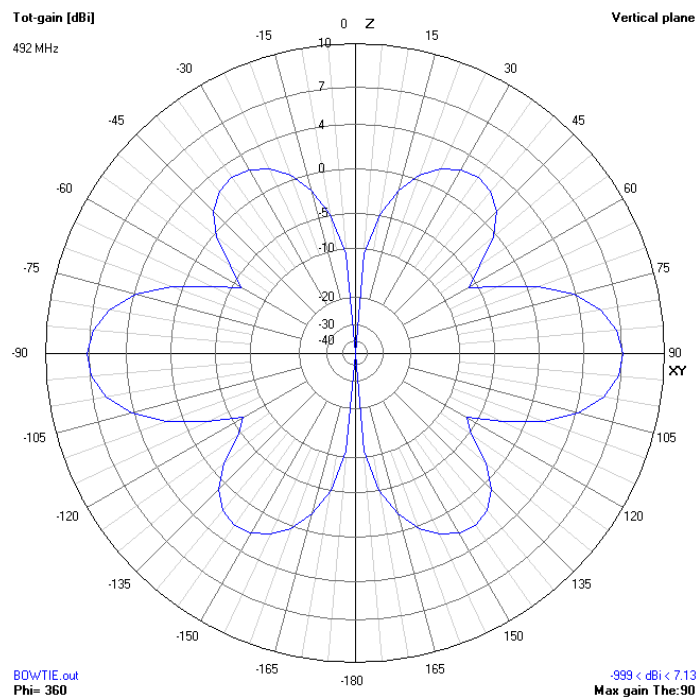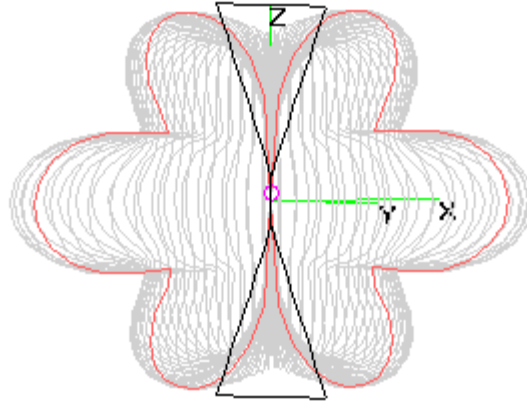Figure 5.19: Polar plot of radiation pattern for a Bow-tie.

47

BOWTIE.out   Tot-gain   492 MHz

Theta : 91   Axis : 1 ft   Phi : 303

Figure 5.20: Antenna radiation pattern/ configuration plot.
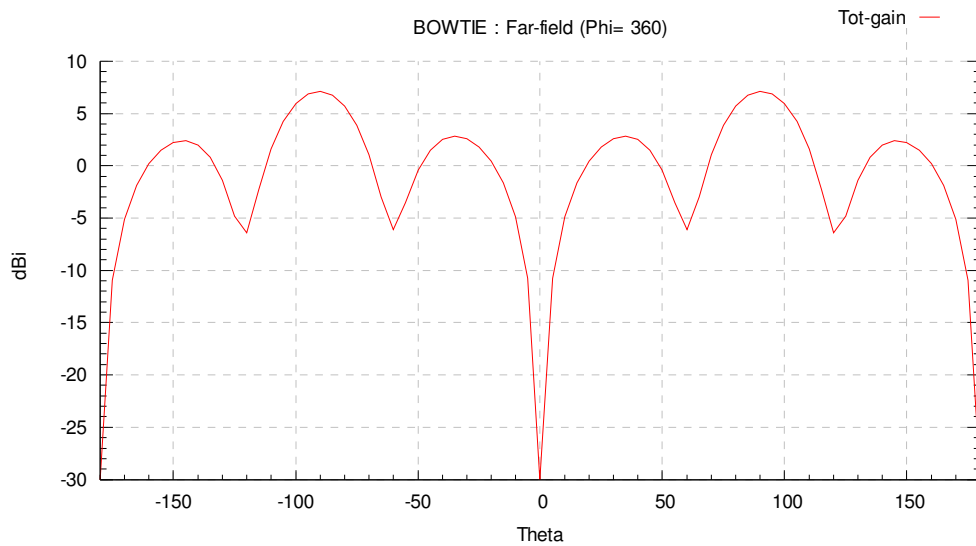
Figure 5.21: Rectangular plot of radiation pattern for a Bow-tie.
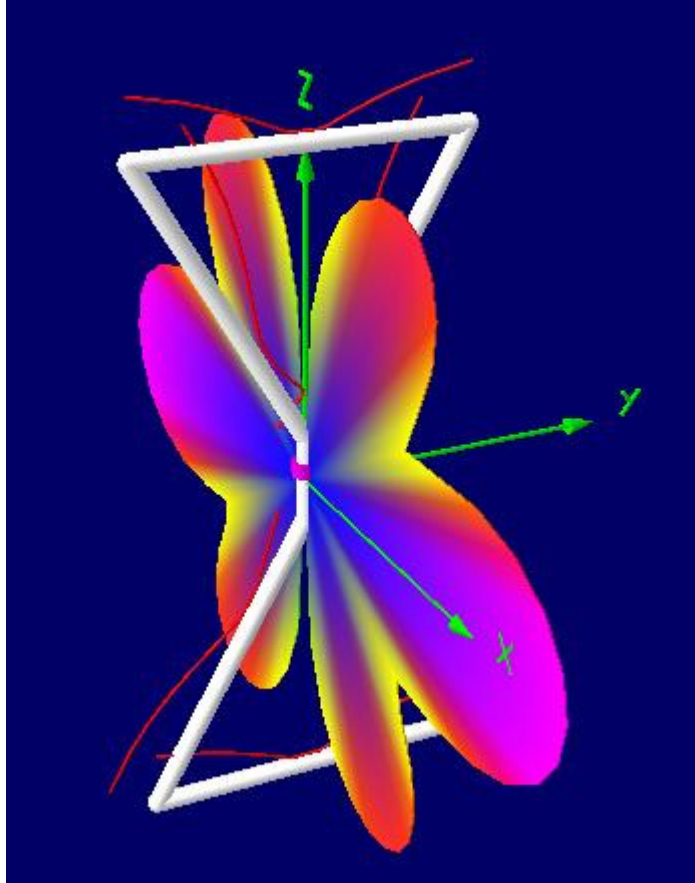
Figure 5.22: Current distribution plot for a Bow-tie.

5.6 Linear Tapered slot antenna

The Linear Tapered slot antenna has been oriented along the Z-axis. In the notepad editor, which is used for providing the antenna dimensions in 4NEC2, the tapered-slot antenna has been divided into 7 wires each consisting of 10 segments. The structural configuration for the Tapered slot antenna is shown below in Figure 5.23.

Theta : 60   Axis : 1 ft   Phi : 10

Figure 5.23: A Linear Tapered slot antenna profile.

The antenna has been fed at the center, at the center of the line joining the two triangles. The frequency of operation for the design constraints posed 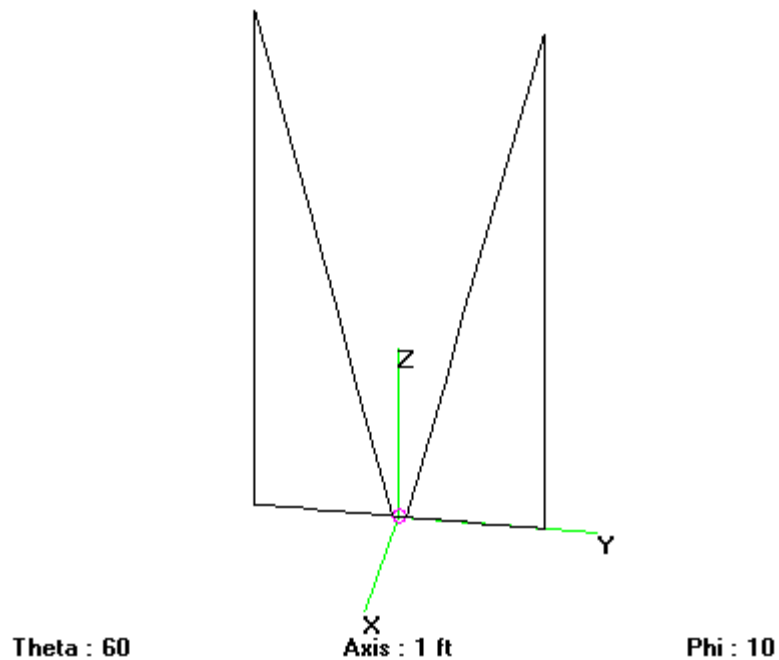by the wing dimensions was 370.5MHz. The Tapered-slot antenna has good gain and radiation patterns at this frequency. The antenna parameters can be seen in Figure 5.24. A pi-matching circuit was used and the antenna has been assumed to be in free space. The polar plot for the radiation pattern is shown in Figure 5.25 below. A radiation pattern plot with the superimposed antenna profile is presented in Figure 5.26. As can be seen from the radiation pattern there are two major lobes oriented along the two tapers. The maximum gain of the tapered slot antenna has been found to be 3.95 dBi (see Figure 5.27).The current distribution along a Tapered slot antenna is shown below in Figure 5.28.
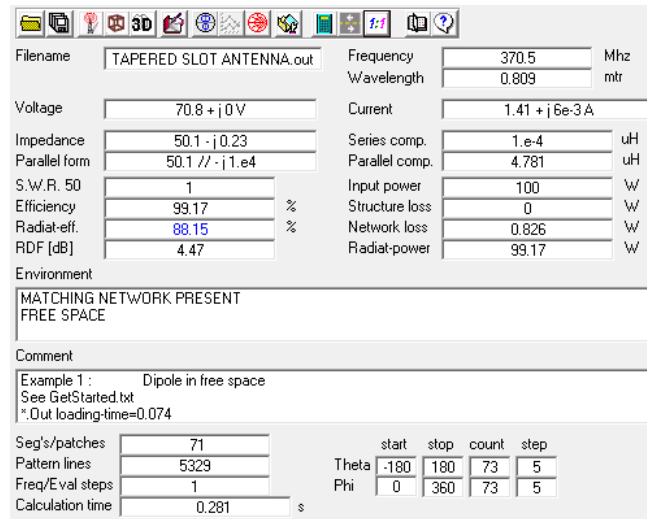
Filename TAPERED SLOT ANTENNA.out

Frequency   370.5   Mhz
Wavelength   0.809   mtr

Voltage   70.8 + j 0 V

Current   1.41 + j 6e-3 A

Impedance   50.1 - j 0.23
Parallel form   50.1 // - j 1.e4

Series comp.   1.e-4   uH
Parallel comp.   4.781   uH

S.W.R. 50   1
Efficiency   99.17   %
Radiat-eff.   88.15   %
RDF [dB]   4.47

Input power   100   W
Structure loss   0   W
Network loss   0.826   W
Radiat-power   99.17   W

Environment

MATCHING NETWORK PRESENT
FREE SPACE

Comment

Example 1 :   Dipole in free space
See GetStarted.txt
*.Out loading-time=0.074

Seg's/patches   71
Pattern lines   5329
Freq/Eval steps   1
Calculation time   0.281   s

	start	stop	count	step
Theta	-180	180	73	5
Phi	0	360	73	5

Figure 5.24: Antenna Parameters for a Linear Tapered slot antenna.

Tot-gain [dBi]
370.5 MHz

Vertical plane

Z

XY

tapered slot antenna.out
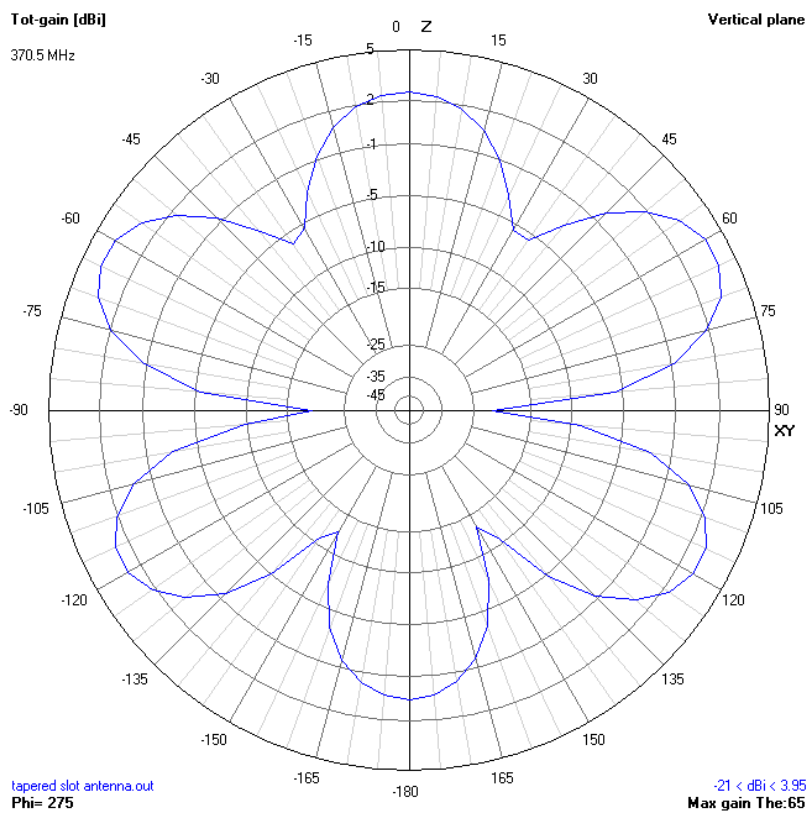Phi= 275

-21 < dBi < 3.95
Max gain The:65

Figure 5.25: Radiation pattern plot for a Linear Tapered slot antenna.
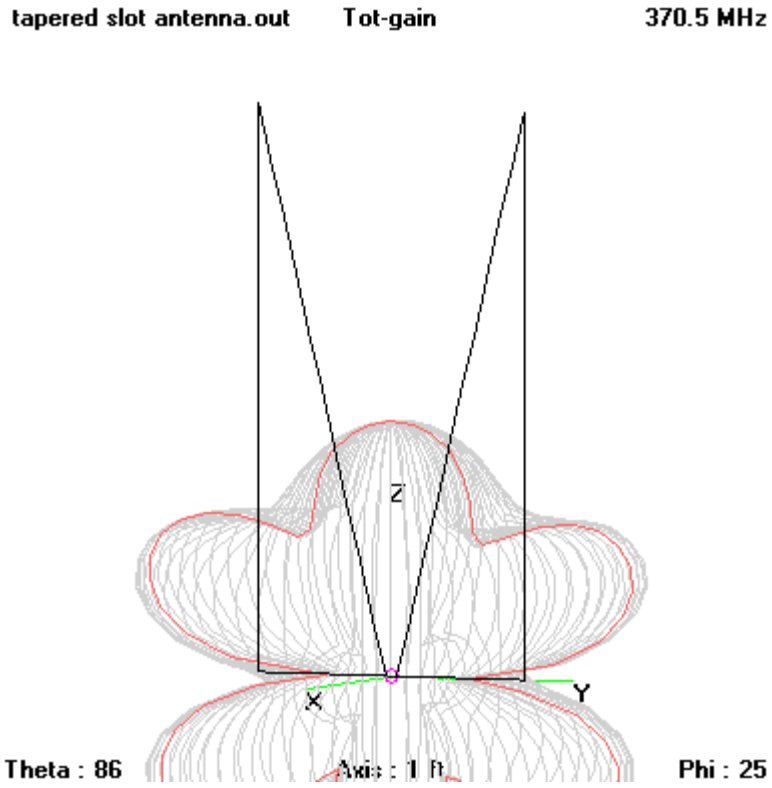
51

Figure 5.26: A radiation pattern/antenna profile plot for a Linear Tapered slot antenna.
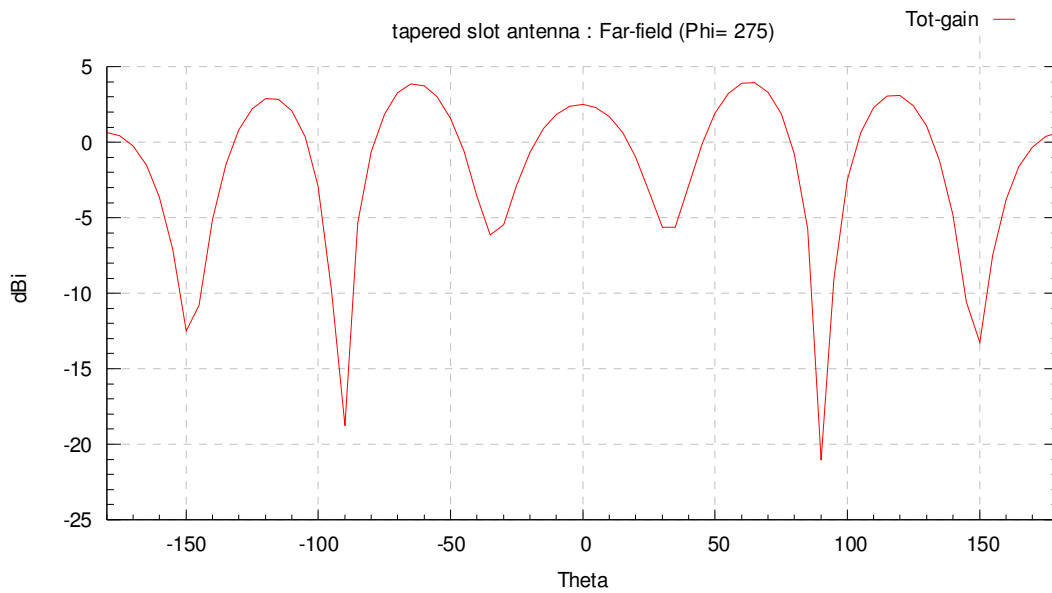

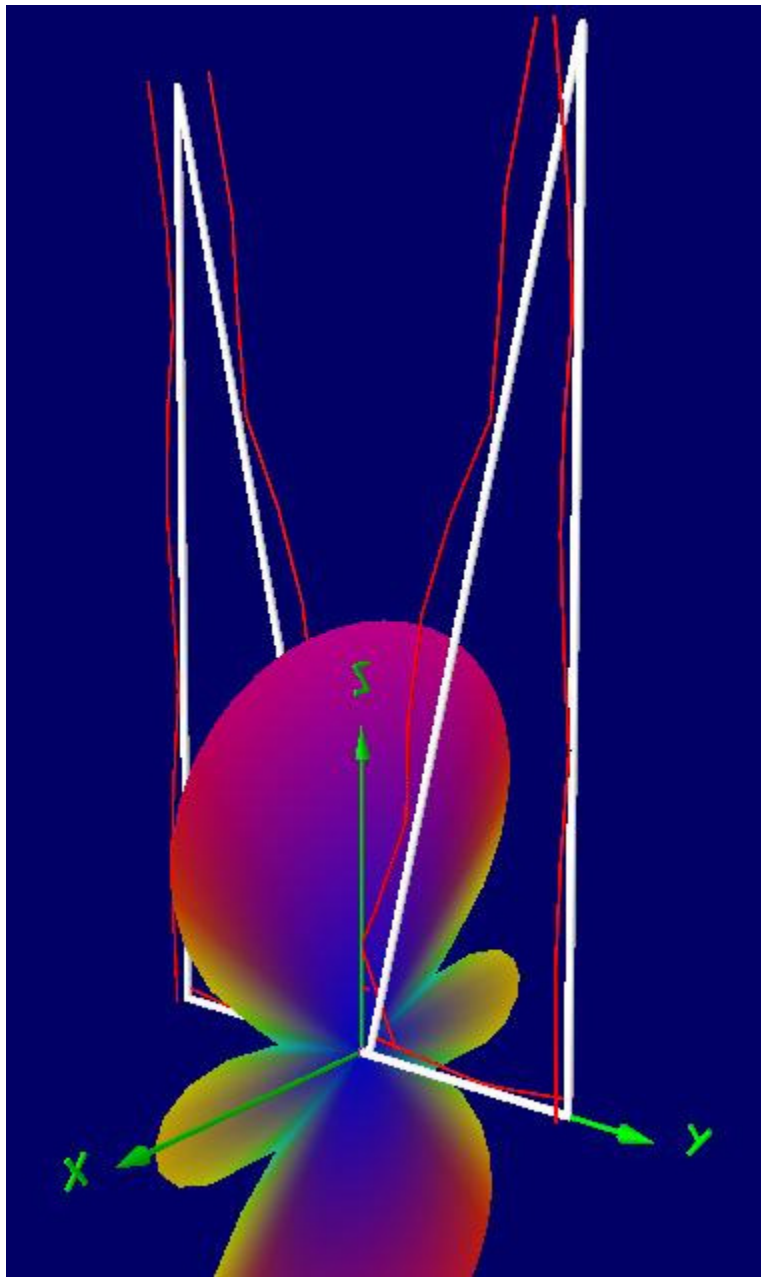Figure 5.27: Rectangular plot for a Linear Tapered slot antenna.

Figure 5.28: Current distribution plot for a Linear Tapered slot antenna.

5.7 Maltese- cross antenna

The Maltese-cross antenna is circularly polarized and has been fed to obtain an excitation of 90 degrees between the two bi-cones. In the notepad editor, which is used for providing the antenna dimensions in 4NEC2, the Maltese-cross antenna has been divided into 14 wires each consisting of 4 segments. The antenna profile as obtained from a 4NEC2 snapshot is as shown in Figure 5.29.
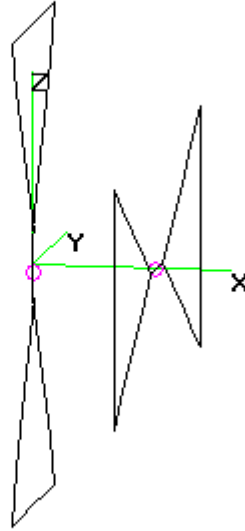
Theta : 80   Axis : 0.2 ft   Phi : 280

Figure 5.29: A Maltese-cross antenna profile, obtained using 4NEC2.

The antenna is made up of two bi-cones which are separated by some distance along the X-axis. The bi-cones are oriented along the Z and Y axis respectively. The antenna has two feed points at the centers of the lines intersecting the two set of triangles. The distance between the bi-cones is equal to the thickness of the inflatable wing available, which is around 0.038 m. A separation of $\lambda/4$ yields a phase difference of 90 degrees and thus, the thickness of the wing (0.038 m) has been equated to $\lambda/4$. As explained in the Chapter 3 the base of each cone has been set to $\lambda/2$ m and the height of each bi-cone to λ m. This choice of dimensions gives a frequency of operation of 1973MHz. It has to be noted that of all the antennas discussed, the Maltese-cross antenna is the only one which is circularly polarized and for which the thickness of the wing has been specifically used. The antenna parameters obtained using 4NEC2 have been presented below in Figure 5.30 and the polar plot for the radiation pattern is shown in Figure 5.31 below. Antenna profile/radiation pattern plot has been presented in the Figure 5.32. As, can be seen from Figures 5.31 and 5.32 the radiation pattern is symmetric along the axis. There are 2 main lobes along with 4 side lobes in the radiation pattern for the Maltese-cross antenna. The maximum gain of the Maltese-cross antenna as shown in the rectangular plot in Figure 5.33 is 5.65 dBi. The current distribution plot has been shown in Figure 5.34 below. The Maltese-cross can be placed anywhere on the inflatable wing. For this example the wing thickness was chosen to provide the 90 degrees phase shift for circular polarization. Other design frequencies could be

54

used for which the thickness is less than λ/4. In those cases, the excitation phase would have to be adjusted accordingly.

Figure 5.30: Antenna parameters for a Maltese-cross.

Figure 5.31: Radiation pattern plot for a Maltese-cross antenna.

Theta : 72   Axis : 0.2 ft   Phi : 287

Figure 5.32: Radiation pattern/Antenna profile plot for a Maltese-cross antenna.

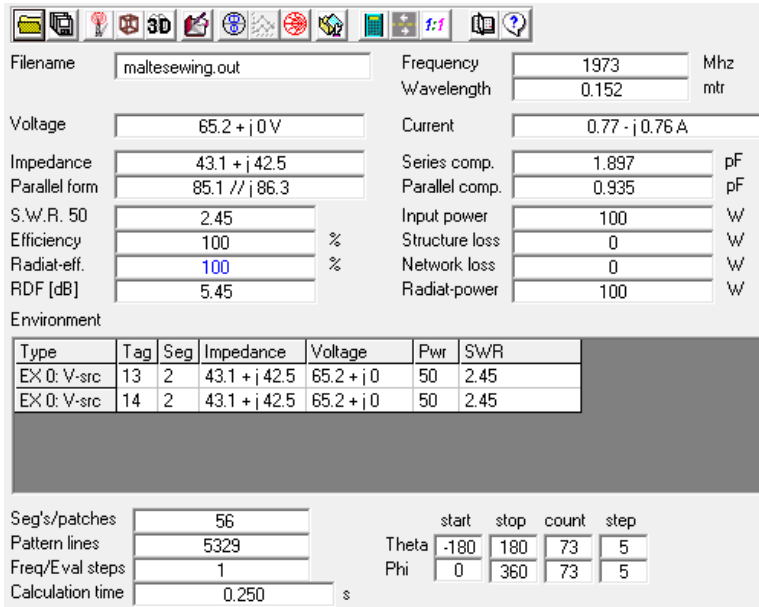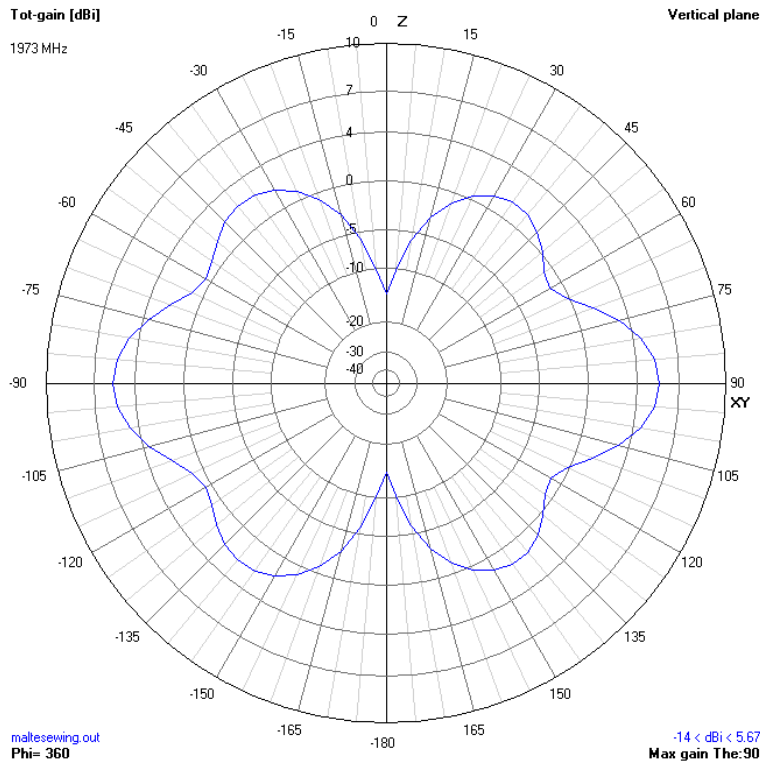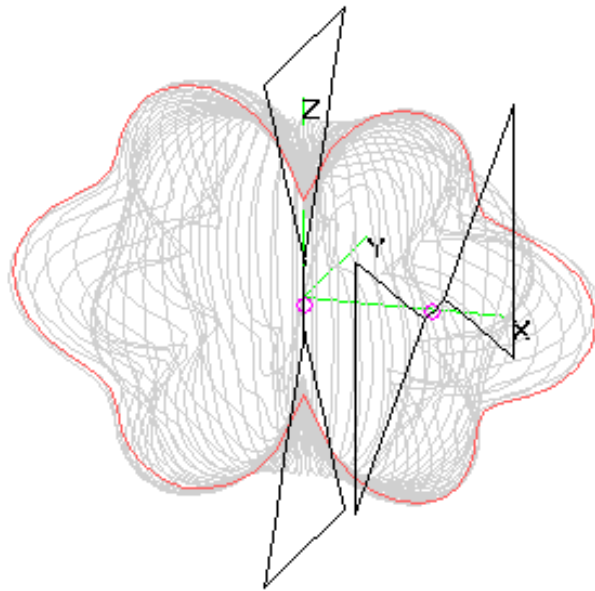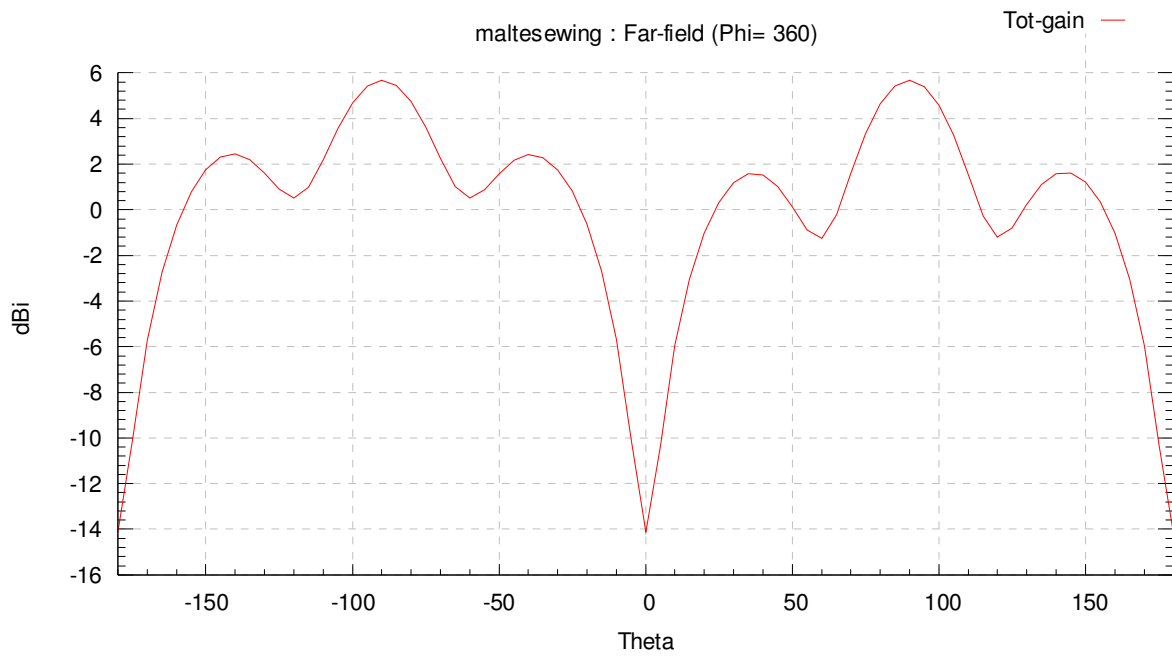Figure 5.33: Rectangular plot for a Maltese-cross antenna.
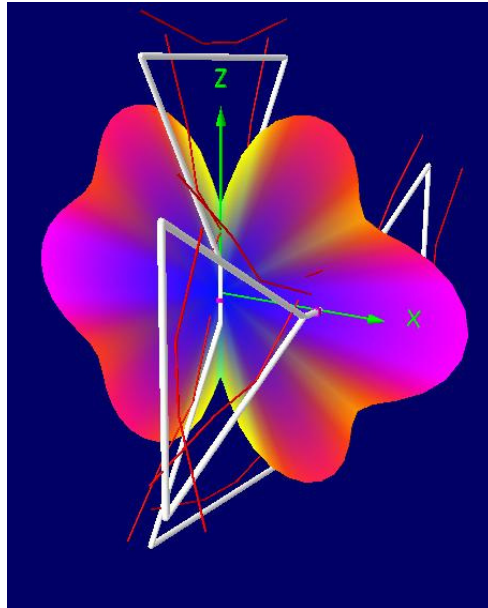
Figure 5.34: Current distribution plot for a Maltese-cross antenna.

5.8 Branch line planar antenna

The Branch line planar antenna has been modeled in the YZ plane. In the notepad editor which is used for providing the antenna dimensions in 4NEC2, the branch line planar antenna has been divided into 34 wires. The wires along the Z and Y direction have been divided into 6 and 4 segments respectively. The antenna profile as obtained from a 4NEC2 snapshot is as shown in Figure 5.33.
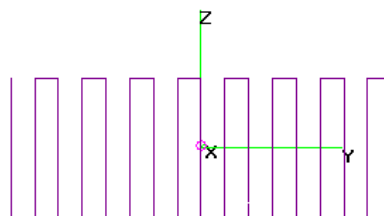
Figure 5.35: A Branch line planar antenna profile.

The antenna is fed at center of the Branch line planar antenna. The antenna is modeled as if in free space. The frequency of operation is 44.93 MHz as the antenna becomes resonant at this frequency and has good gain and radiation patterns. Figure 5.34 below gives all the design parameters as obtained from the 4NEC2 window. An L-matching circuit was used here. The radiation pattern for this antenna as obtained from 4NEC2 is presented in Figure 5.35. As, can be seen from Figure 5.35 the radiation pattern obtained is fairly broad. The antenna/radiation pattern plot has been presented in Figure 5.36. The maximum gain obtained is 6.9dBi and can be seen in the rectangular plot in Figure 5.37. The current distribution plot is shown in Figure 5.38 below. Except for the Branch line planar antennas, all the other antennas that were presented had the frequency of operation in the VHF and UHF range. As explained in Chapter 4, because of the coupling between adjacent sections, the antenna became resonant only at 44.93 MHz as opposed to straight-wire mathematically calculated frequency of 12.4275 MHz for the wing dimensions. A coaxial cable or thin wires can be used to run around the spars and form a branch line planar antenna. Substrate materials with good flexibility and dielectric properties can also be used to build these antennas. A comparison between all these antennas and their parameters is shown in the following section.

Figure 5.36: Antenna parameters for Branch line planar antenna.

Figure 5.37: Radiation pattern for a Branch line planar antenna.

Figure 5.38: Antenna/ radiation pattern plot for a Branch line planar antenna.

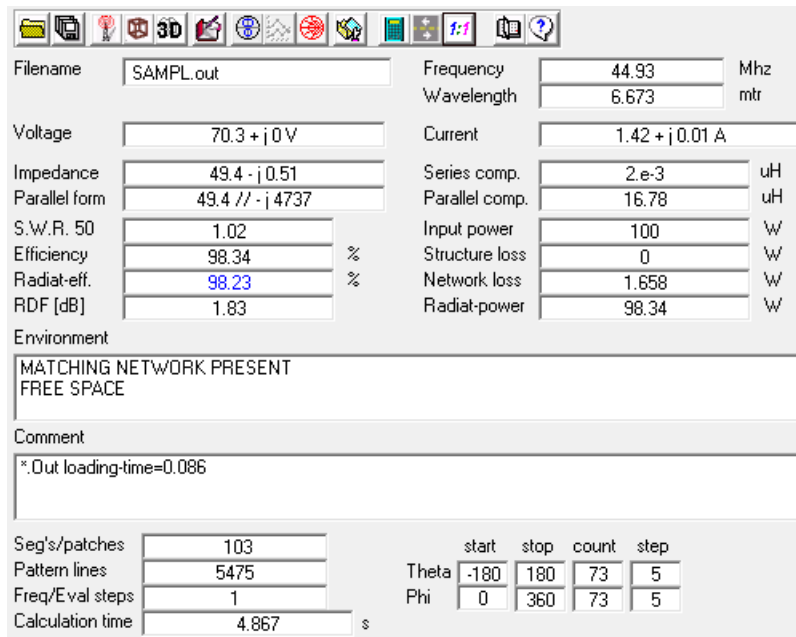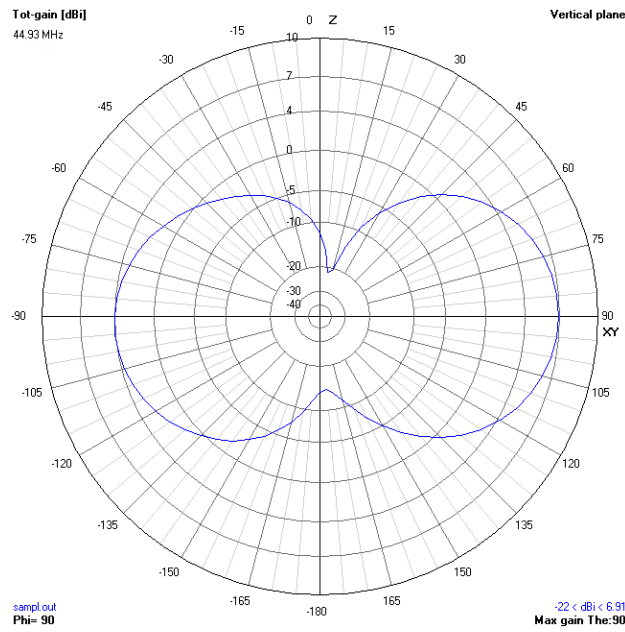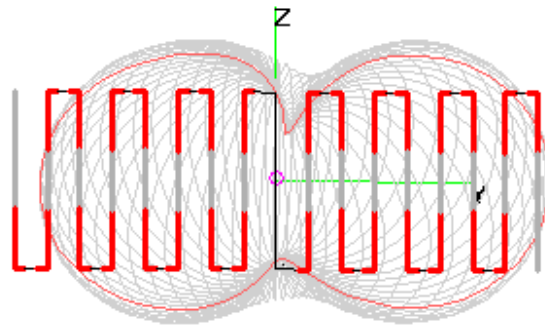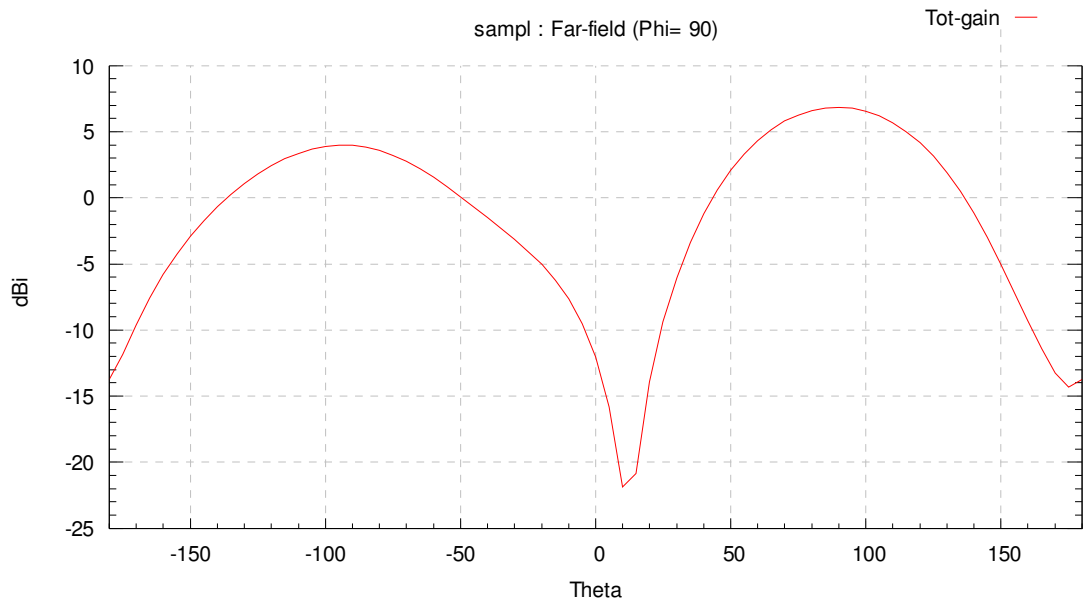Figure 5.39: Rectangular plot for a Branch line planar antenna.
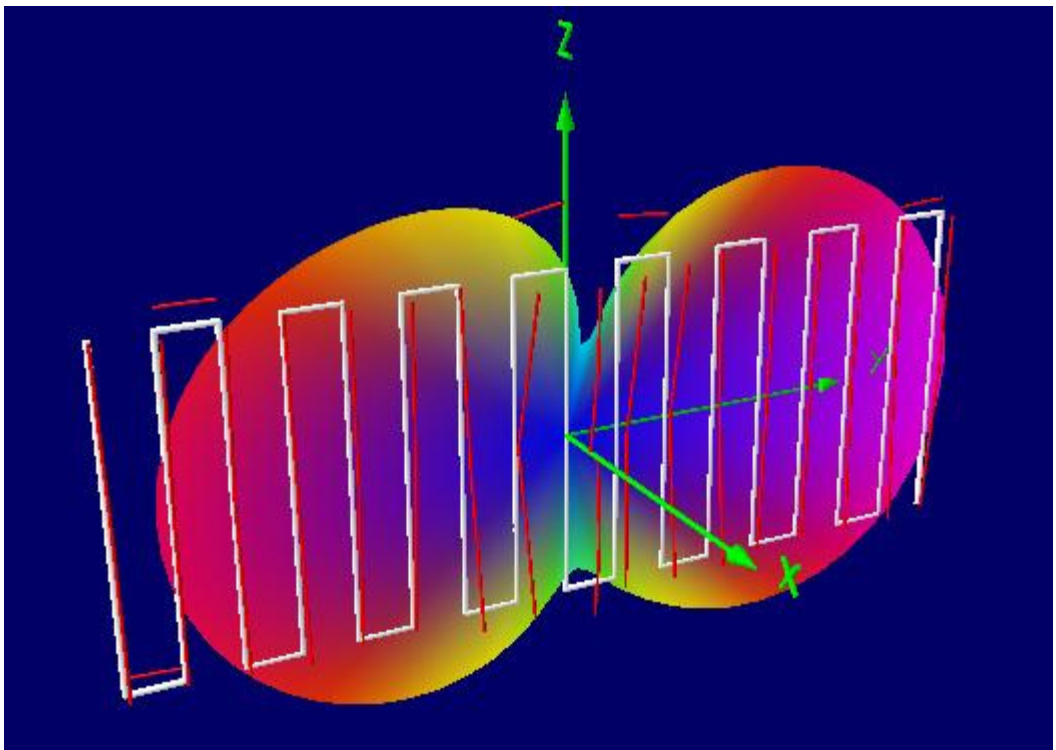
Figure 5.40: Current distribution for a Branch line planar antenna.

5.9 Comparison of antenna parameters

Table 5.1: Comparison of various antenna parameters

Antenna	Half-wave dipole antenna	Three-element Yagi-Uda antenna	Bow-tie antenna	Linear Tapered slot antenna	Maltese-cross antenna	Branch line planar antenna
Frequency of operation	900 MHz	900 MHz	492 MHz	370.5 MHz	1973 MHz	44.93 MHz
Radiation pattern	Doughnut pattern	Endfire pattern	Has 2 main lobes along with a few side lobes	Has 2 major lobes in the direction of the tapers	Has 2 major lobes along with side lobes	Fairly broad
Maximum Gain (in dBi)	2.1	8.5	7.13	3.95	5.65	6.9
Input impedance (Real part, in Ohms)	77.2	41.4	49.9	42.9	43.1	7.7
Antenna array	Not possible	Possible and results are a little better with arrays	Not possible	Not possible	Not possible	Not possible

As, can be seen from the comparisons, for a lower frequency of operation, branch line planar antennas can be chosen. For higher gain, Bow-tie and Yagi- Uda are suitable. The antenna with the best input impedance is the Bow-tie.

5.10 Conclusions

The simulation results for all the antenna configurations have been discussed in depth and a comparison of all these antennas along with their parameters was shown. Most of these antennas can be used for inflatable wings as the wings are non-conducting and relatively RF transparent. The programs Wirecode and 4NEC2 used for simulation have been explained. From the simulation results it is clear that the antennas can be divided into two classes.

- The antennas designed for higher VHF, UHF range and the antenna designed for lower VHF range.
- The antennas which are more directive and ones with lower gain.

Depending on the requirement, an antenna configuration can be selected to provide any one the features or a mix of them.

CHAPTER 6- EFFECT OF FLEXIBILITY ON ANTENNA PARAMETERS FOR THE BRANCH LINE DIPOLE

6.1 Introduction

The inflatable wing is somewhat flexible and during flight it deflects through various degrees at the ends and at the center. The antenna which is placed on or in the inflatable wing also deflects along with the wing and this leads to slight variation in performance parameters. This chapter will discuss the effect of flexibility on the branch line antenna parameters, like input impedance and radiation patterns.

There are aerodynamic limits to the amount an inflatable wing can flex and maintain stable flight. Typical parameters for the deformation of the inflatable wing are a maximum of ± 6 degrees at the ends [20]. This deformation is because of the movement of the wing along the X-direction during flight.

6.2 Wing tip deflection

The antenna deflects by a maximum of ± 6 degrees at the ends and the antenna configuration resembles a semi-cubical parabola. Figure 6.1 gives the profile of the Branch line planar antenna for the mode obtained as a result of the flexing wing along the X-direction. The program 4NEC2 was used for modeling the distorted antenna. The antenna was divided into 34 wires. In this mode the maximum displacement of the wing at the ends along the X-axis is about 6cm.
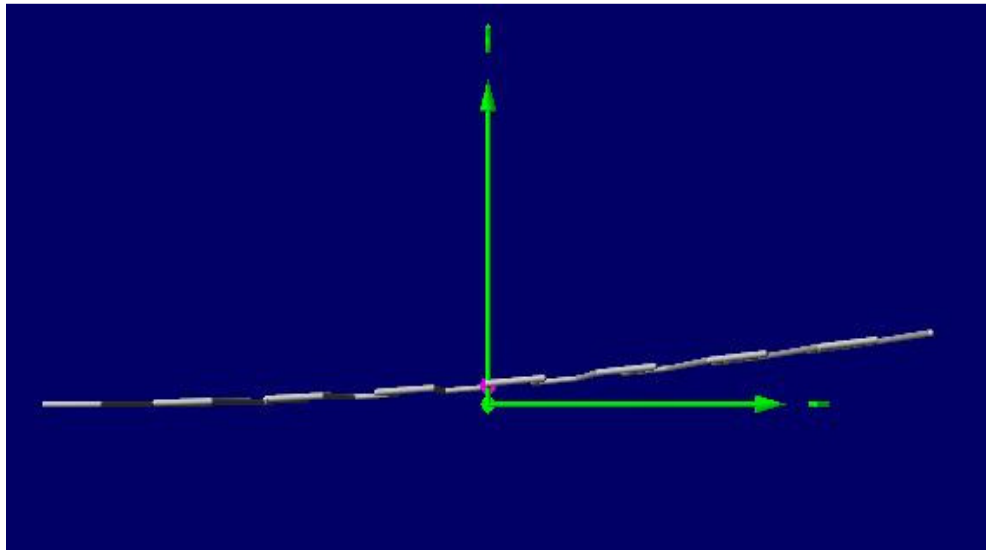

Figure 6.1: Antenna profile of a Branch line planar antenna for a deflection of 6 degrees at the end.

The radius of each wire is 1 mm and the antenna is assumed to be in free space. The frequency of operation is 44.93 MHz which was the original design frequency for this antenna. Figure 6.2 below gives all the design parameters as obtained from the 4NEC2 window. A Pi-matching circuit was used. The radiation pattern for this antenna, when compared to that for an undistorted antenna obtained using 4NEC2, is presented in Figure 6.3. The antenna/ radiation pattern plot is shown in Figure 6.4. There is not much of a change in the radiation pattern when compared to the radiation pattern of an undistorted Branch line antenna. The input impedance in this case is 7.36Ω as opposed to 7.7Ω for an undistorted antenna. The maximum gain obtained here is 6.2dBi and can be seen in the rectangular plot in Figure 6.5. The maximum gain for an undistorted branch line antenna as presented in Chapter 5 was 6.9 dBi. The current distribution plot is shown in Figure 6.6 below. The antenna is fed at center of the Branch line planar antenna. Given the mechanical aerodynamic constraints on the wing shape perturbation, there is not a dramatic change in antenna parameters because of this mode of wing deflection.
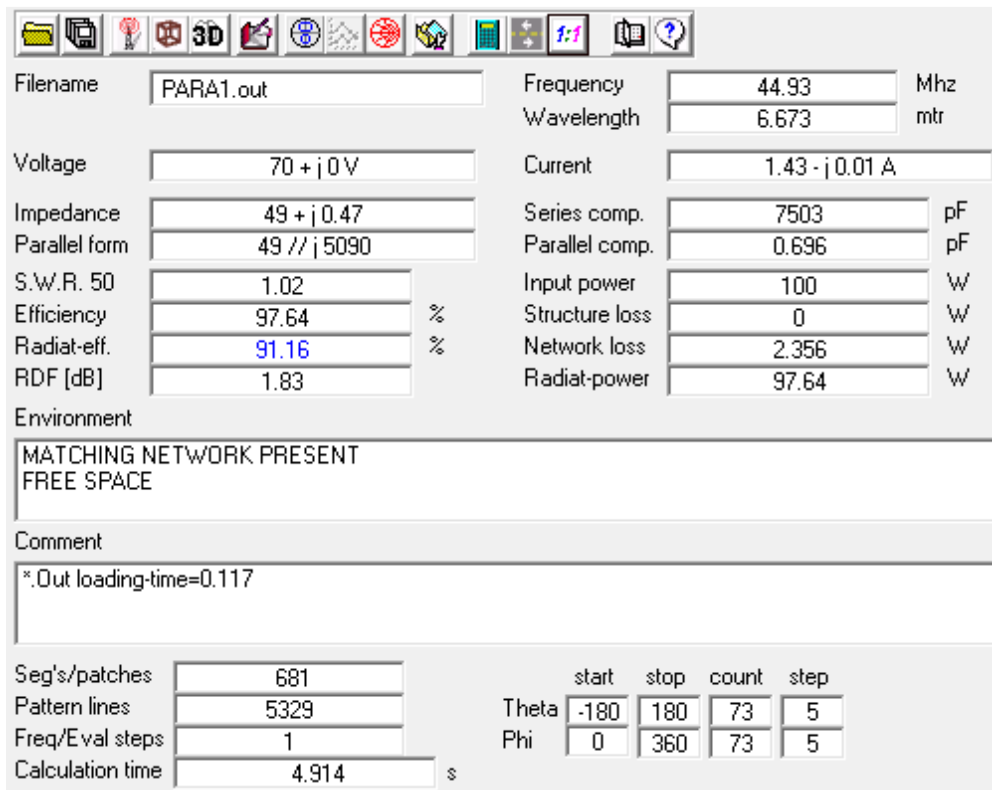
Figure 6.2: Antenna parameters for a Branch line planar antenna for the mode of operation due to deflection at the ends.

Figure 6.3: Comparison of Radiation Pattern for (a) Undistorted Branch line planar antenna (b) Branch line planar antenna in the mode of operation, due to deflection at the ends.
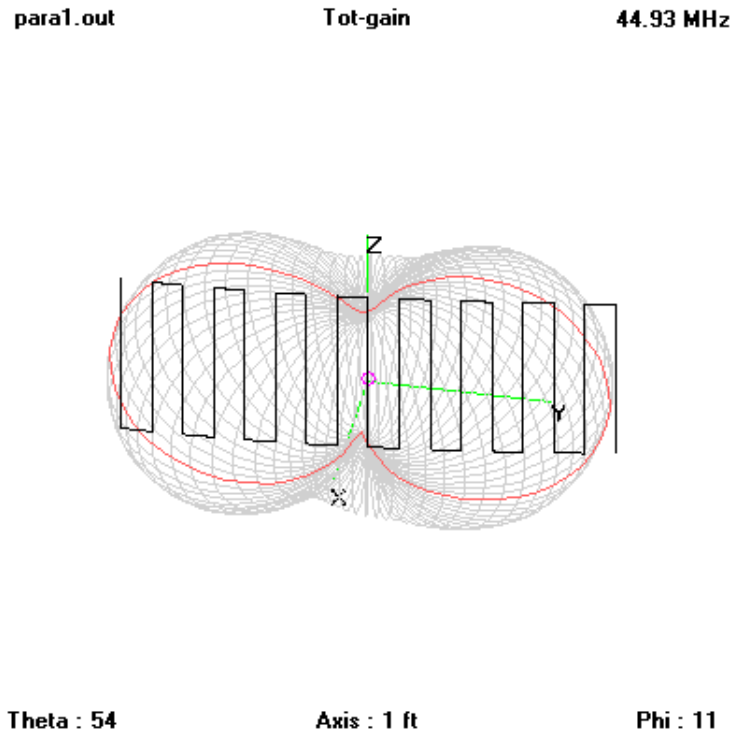
Figure 6.4: A superimposed antenna/radiation pattern plot for a branch line antenna in the mode of operation due to deflection at the ends.
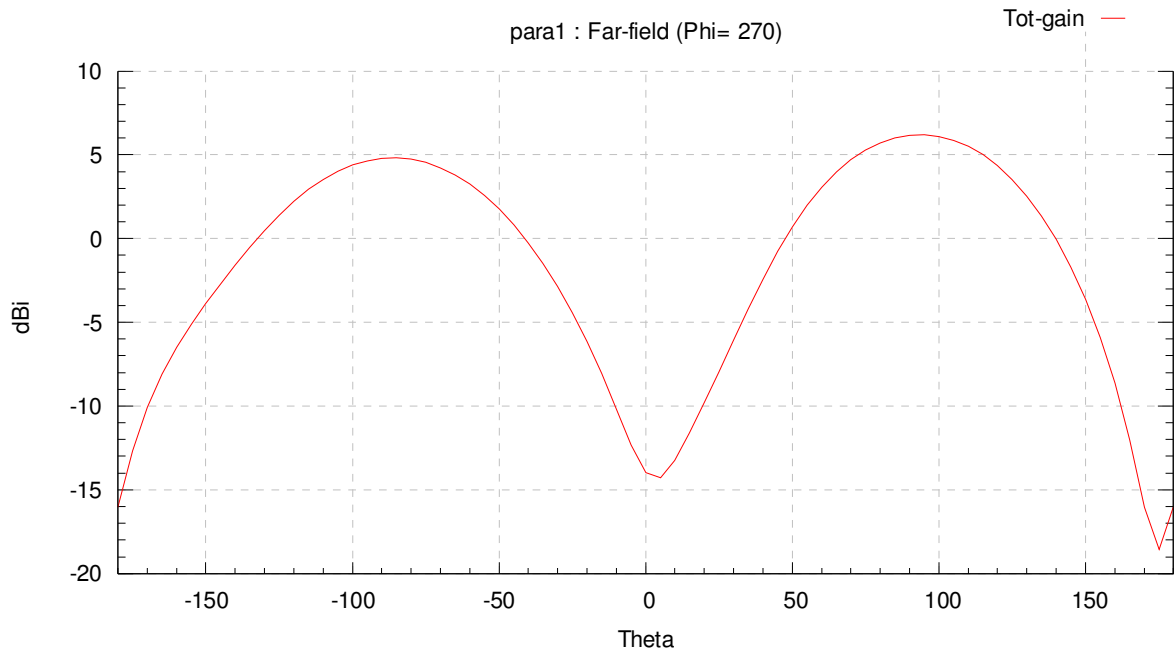
Figure 6.5: Rectangular plot for a Branch line planar antenna in the mode of operation due to deflection at the ends.
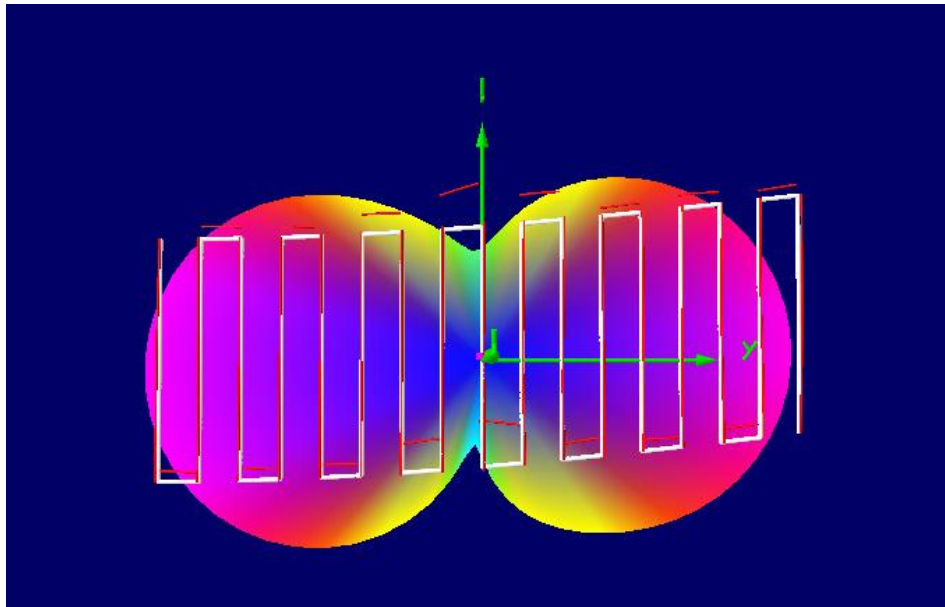
Figure 6.6: Current distribution for a Brach line planar antenna in the mode of operation due to deflection at the ends.

6.3 Wing center deflection

For a second mechanical mode, the inflatable wing can deflect in the center resulting in the form of an arc during flight. Figure 6.7 gives the profile of the Branch line planar antenna which is deflected in the center. The program 4NEC2 is again used here and the antenna has been divided into 34 wires.
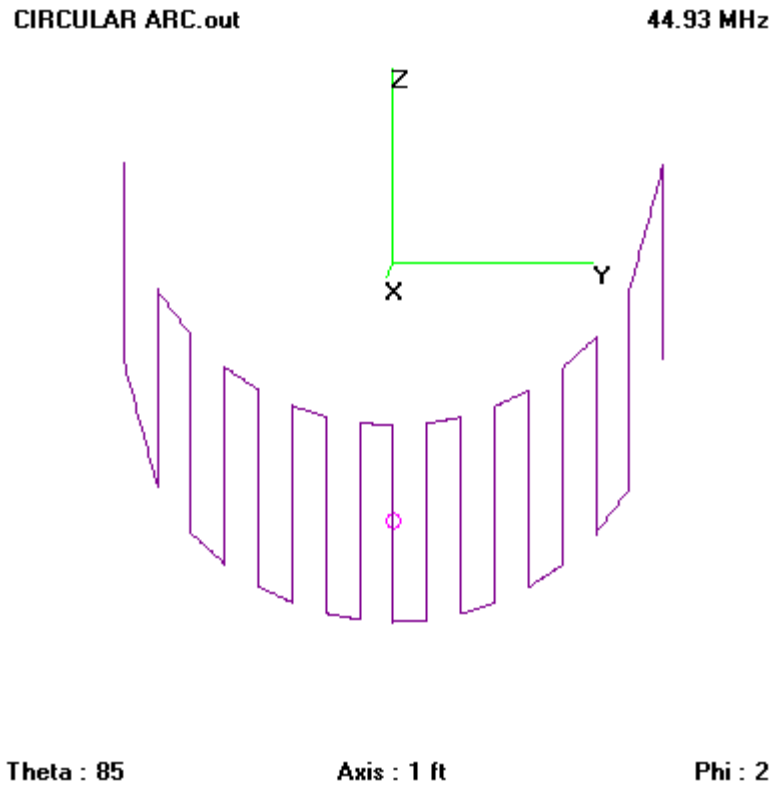
Figure 6.7: Exaggerated antenna profile of a Branch line planar antenna with center deflection.

The radius of each wire is 1 mm and the antenna is assumed to be in free space. The center deflects by a maximum of 10 cm here from its original undistorted position. The frequency of operation is 44.93 MHz which was the original design frequency. Figure 6.8 below gives all the design parameters as obtained from the 4NEC2 window. A Pi- matching circuit was used here. The radiation pattern for this antenna, when compared to that for an undistorted antenna obtained using 4NEC2, is presented in Figure 6.9. There is a considerable deterioration of the radiation pattern when compared to the radiation pattern of an undistorted branch line antenna. The input impedance in this case is 10.3Ω as opposed to 7.7Ω for an undistorted antenna. The antenna/radiation pattern plot is presented in the Figure 6.10 below. The maximum gain obtained here is 6.62 dBi and can be seen in the rectangular plot in Figure 6.11. The maximum gain for a normal Branch line antenna as presented in Chapter 5 was 6.9 dBi. The current distribution plot is shown in Figure 6.12 below. The antenna is fed at center of the

Branch line planar antenna. Thus, there is a moderate change in antenna parameters because of the effect of the wing deflection in the center.
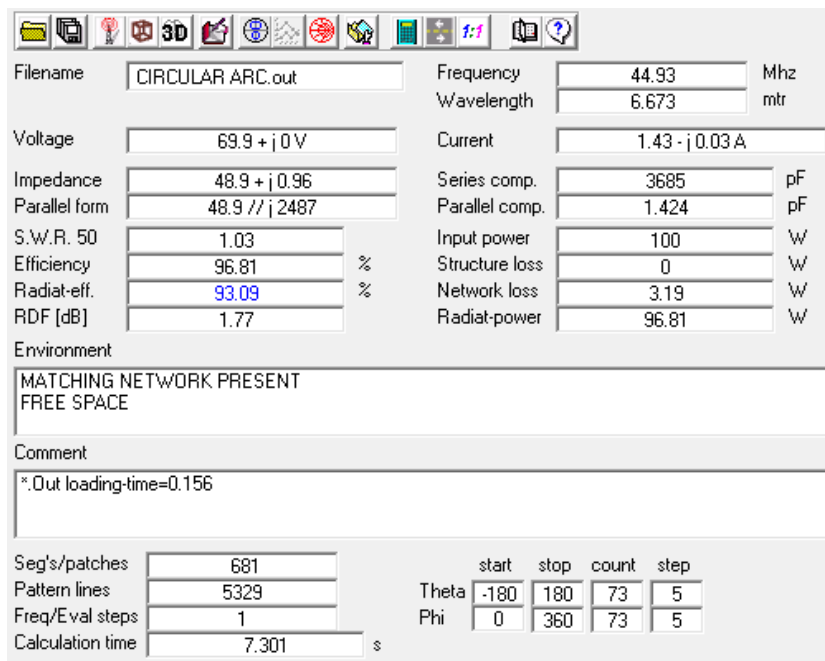
Figure 6.8: Antenna parameters for a Branch line planar antenna with center deflection.
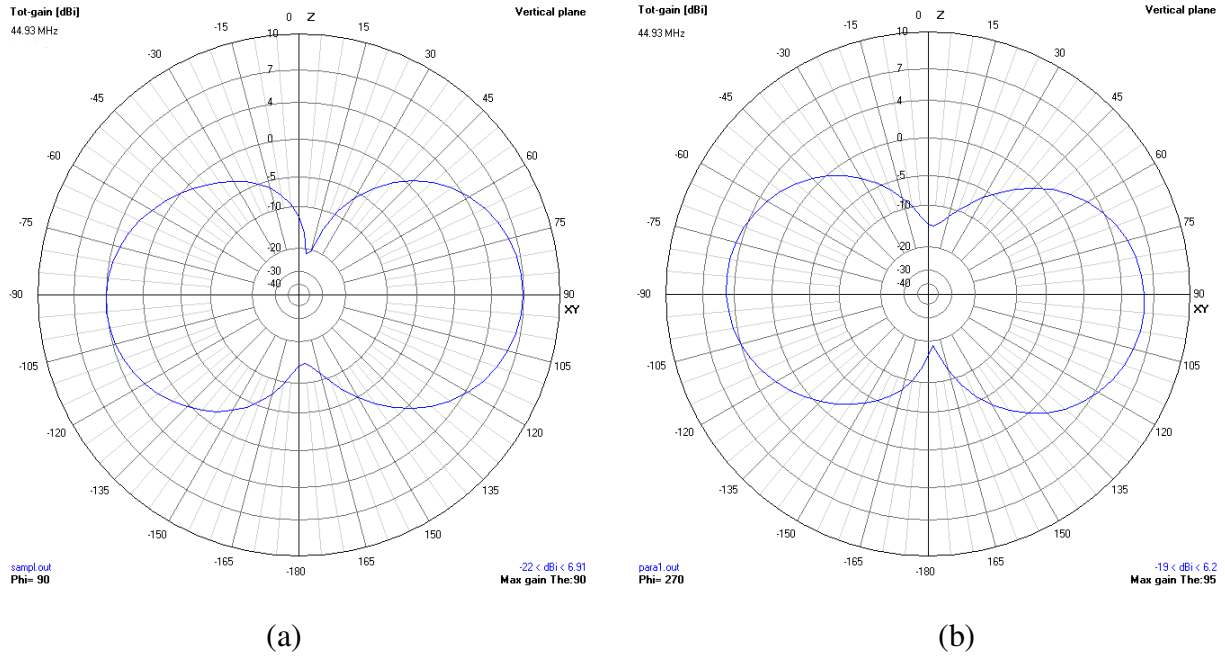

(a)   (b)
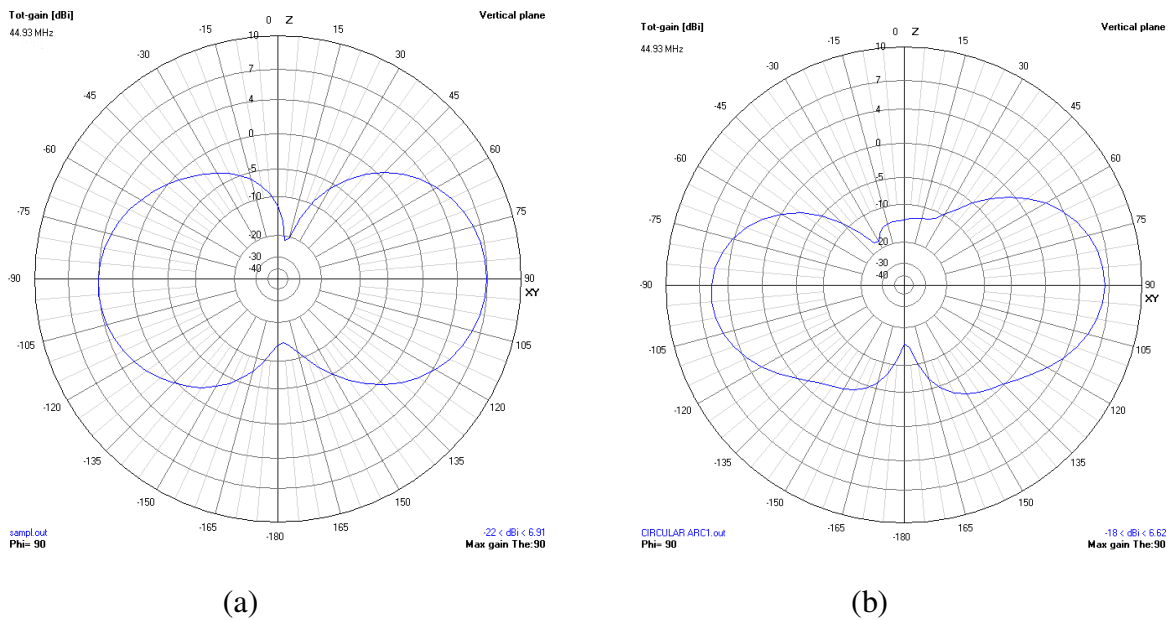
Figure 6.9: Comparison of Radiation Pattern for (a) Undistorted Branch line planar antenna (b) Branch line planar antenna, with center deflection.

CIRCULAR ARC1.out   Tot-gain   44.93 MHz
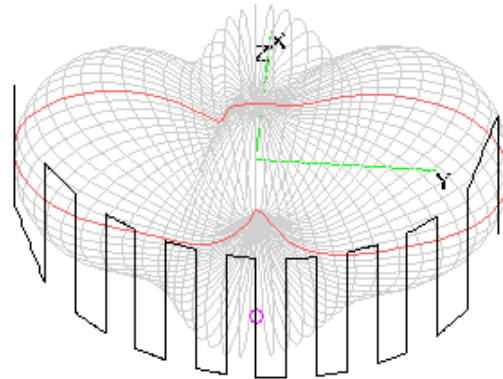
Theta : 138   Axis : 1 ft   Phi : 355

Figure 6.10: A superimposed antenna/radiation pattern plot for a branch line planar antenna with center deflection.
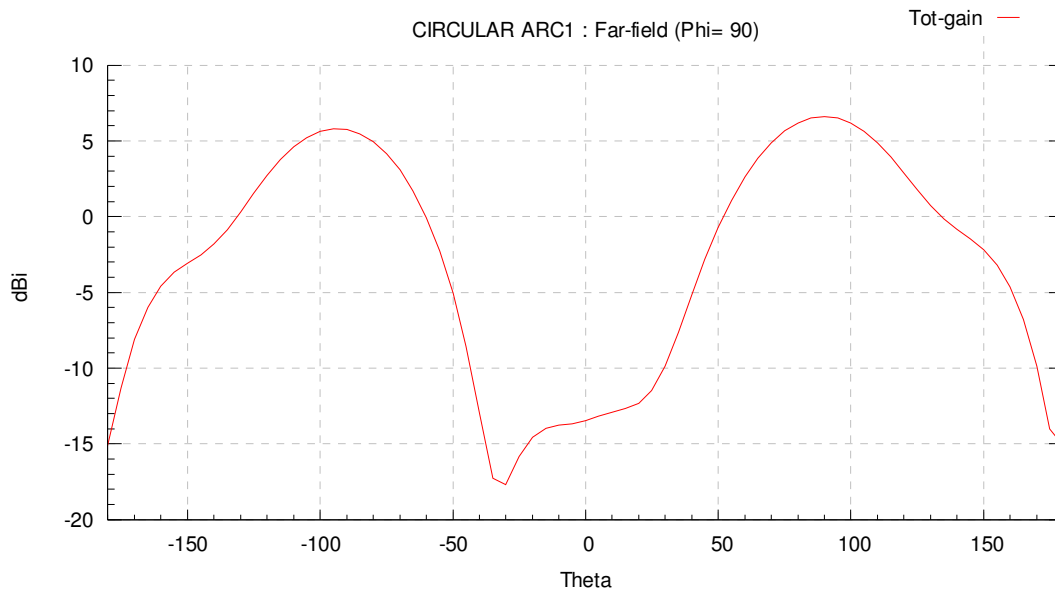
Figure 6.11: Rectangular plot of a Branch line planar antenna with center deflection.
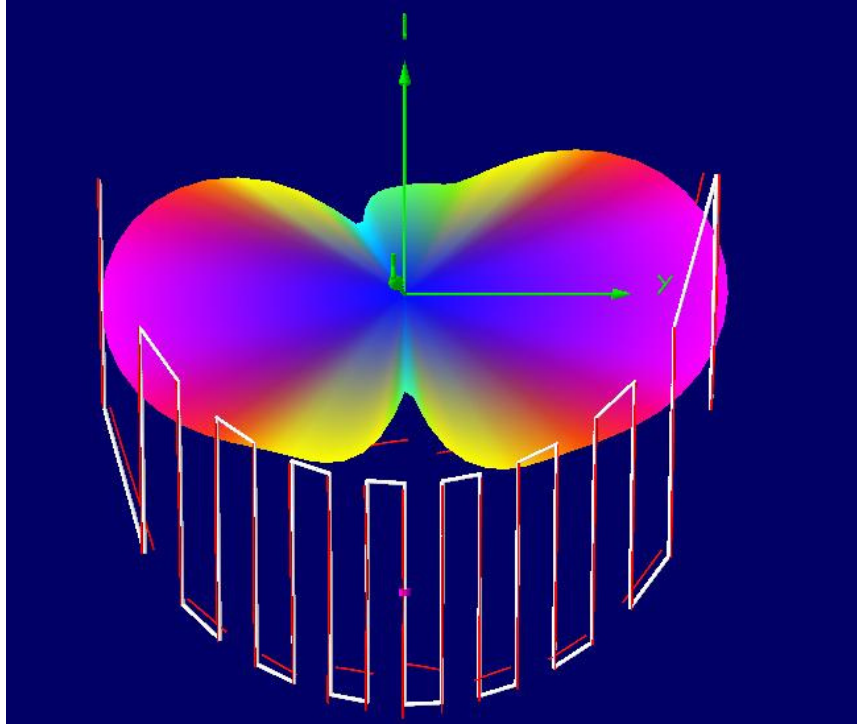
Figure 6.12: Current distribution of a Branch line planar antenna with center deflection.

6.4 CONCLUSIONS

The simulation results for the Branch line planar antenna have been thoroughly discussed for two wing deflection modes obtained due to the effect of flexibility at the center and at the ends. Thus, by looking at the results it can be safely concluded that the antenna parameters will not significantly change because of deflection at the ends of the inflatable wing during flight. However, when the wing is in the shape of a circular arc a noticeable, yet still reasonable, change in the antenna gain, input impedance and radiation pattern can occur. The wing tip deflection changes are not as bad as the wing center deflection changes as the point of feed at the center, is marginally displaced from its initial position for wing tip deflection.

CHAPTER 7- SUMMARY & CONCLUSIONS

The thesis has met the objectives set forth in the introductory chapter. A set of antennas which can be deployed with the inflatable wings have been identified and analyzed. These antennas were modeled to make use of the structure of the wing. Several of them can operate at the higher VHF and UHF frequencies and above. In the process, the branch line planar antenna, operable at lower VHF range, were developed and can serve as a basis for stimulating future concept ideas.

7.1 Summary

The first chapter of the thesis gave a brief background of deployable wings, inflatable wings being one type, and highlighted how inflatable wings could be of use in MARS exploration. The motivation behind the thesis and the objectives and contributions of the work were clearly spelled out. The potential impact of the thesis was also discussed. Chapter 2 gave a theoretical discussion of antenna concepts required for working on this thesis. Chapter 3 was dedicated to antenna types which were operable at the higher VHF and UHF frequency range. This chapter covered the Half-wave dipole, Yagi-Uda, Bow-tie, Linear Tapered-slot and Maltese-cross antennas. A detailed analysis of the antenna profiles, dimensions and the position on the inflatable wing was provided.

Chapter 4 exclusively discusses Branch line planar antennas. The chapter discusses how this set of antennas effectively uses the structure of the wing to give an efficient antenna operating at the lower VHF frequency. The guidelines for obtaining antenna dimensions have also been provided. Chapter 5 provides the simulation results and explanation for all the antennas discussed in the Chapters 3 and 4 in detail. A comparison of all the antennas is also done at the end. Chapter 6 examines how the flexibility of the wing affects the parameters of the branch line antenna. Two main cases of deflection at the ends and at the center, respectively, have been discussed. Detailed simulation results have also been presented to explain the effect of the flexibility of the wing on the antenna parameters. It was shown that within the structural aerodynamic displacement limits, the flexing had a minimal effect on the branch line antenna performance.

7.2 Contributions

- The structure of the inflatable wing was used to design deployable antennas.
- Guidelines for the dimensions of the branch line antennas were provided. These dimensions give acceptable radiation pattern, gain, input impedance and other antenna properties.
- A set of deployable antennas appropriate for an inflatable wing operating at the higher VHF and UHF, or at the lower VHF range, have been constituted. These antennas are all structurally feasible, conformal and flexible.

- As the wing flexes during flight, the antenna deployed on the wing fluctuates, too, thereby changing the antenna parameters. A chapter has been dedicated to showcase the effects the flexibility of the wing can have on the branch line antenna parameters. The application of the branch line dipole allows for efficient antenna communication at frequencies lower than possible with more conventional designs.

7.3 Directions and Possibilities for future work

- The idea of integrating the structure of the inflatable wing with that of an antenna has many advantages without compromising the antenna parameters. More antennas on this concept can be evaluated in the future.
- Research can be focused on using various kinds of flexible substrates for designing the branch line and other antennas.
- The concept of tensairity, which is a new lightweight structural concept, can be worked with and integrated with structurally feasible deployable antenna designs.

References

[1] Leonardo Da Vinci's "flying machines",
     http://www.angelfire.com/electronic/awakening101/leonardo.html.

[2] Ornithopter notes,
    http://www.daviddarling.info/encyclopedia/O/ornithopter.html.

[3] Jim Walker military launcher for folding wing A-J army interceptor,
    http://www.americanjuniorclassics.com/interceptor/militarylauncher.htm.

[4] TOW-2 Heavy Anti Tank Missile-Army technology,
    http://www.army-technology.com/projects/tow/.

[5] J. Pike, "A-3 / EA-3B Skywarrior," April 2004,
    http://www.globalsecurity.org/intell/systems/ea-3.htm.

[6] Mustang-Aeronautics, "Folding Wing," April 2007,
    http://www.mustangaero.com/Mustang%20II/FoldingWing.html.

[7] J. Anderson, "The Crosbie Folding Wing," December 1998,
    http://freespace.virgin.net/shadow.owners/anderson.htm.

[8] Marion L. Carroll, "WASP", May 1998,
    http://web.mit.edu/aeroastro/www/labs/ICE/projects/wasp.html

[9] D. Cadogan, W. Graham and T. Smith, "Inflatable and Rigidizable Wings for Unmanned
     Aerial Vehicles", 2nd AIAA "Unmanned unlimited" systems, San Diego, CA, Sept 2003
     AIAA 2003-6630.

[10] Research Channel, "Flying on Air: The Science of Inflatable Wings".

[11] Robert E. Collin, Antennas and Radiowave Propagation, USA: McGraw-Hill,
     Inc., 1985

[12] C. A. Balanis, Antenna Theory: Analysis and Design, 2nd Ed. New York:
     John Wiley & Sons, Inc., 1997.

[13] W. L. Stutzman and G. A. Thiele, Antenna Theory and Design, 2nd Ed.
     USA: John Wiley & Sons, Inc., 1998.

[14] Dr. William T. Smith, EE 522 notes, University of Kentucky

[15] The Toronto soaring club, 2004.
     http://www.toronto-soaring.ca/about.html

[16] Carl E. Baum and Dean I Lawry, "A conical slot antenna and related antennas suitable for use with an aircraft with inflatable wings", sensor and simulation notes, note 496, March 2005.

[17] Peng-Thian Teo, Kian-Seng Lee and Chiang-Kwang Lee,"Maltese-cross coaxial balun-fed antenna for GPS and DCS 1800 mobile communication", IEEE transactions on vehicular technology, Vol 52, No.4, July 2003 779.

[18] Kin-Lu Wong, Planar antennas for wireless communications, 1st edition,
John Wiley & Sons, Inc., 2003.

[19] Arie Voors, "4NEC2 antenna modeler and optimizer," May 2005,
http://home.ict.nl/~arivoors/

[20] In consultation with Dr. Suzanne Weaver Smith, professor, Mechanical Engineering, University of Kentucky.

[21] Chris Bowick, RF circuit design, 1st edition,
Newnes publishers, 1997.

Vita

Personal
Date and place of birth: 25th February 1986, Hyderabad, Andhra Pradesh, India

Education
Bachelor of Technology (B.Tech) in Electronics and communication engineering, May 2007
Jawaharlal Nehru technological University
Hyderabad, Andhra Pradesh, India